Application of novel pharmaceutical carrier systems to oral insulin delivery

Application of novel pharmaceutical carrier systems to oral insulin delivery

Takahiro Goto

CONTENTS

LIST OF PUBLICATION

1. Mucosal insulin delivery systems based on complexation polymer hydrogels: effect of particle size on insulin enteral absorption. Mariko Morishita, Takahiro Goto, Nicholas A. Peppas, Jeffery I. Joseph, Marc C. Torjman, Carey Munsick, Koji Nakamura, Tetsuo Yamagata, Kozo Takayama, and Anthony M. Lowman. Journal of Controlled Release, 97, 115–124 (2004). <presented in Chapter 1 of this dissertation>

2. Novel oral insulin delivery systems based on complexation polymer hydrogels: Single and multiple administration studies in type 1 and 2 diabetic rats. Mariko Morishita, Takahiro Goto, Koji Nakamura, Anthony M. Lowman, Kozo Takayama, and Nicholas A. Peppas. Journal of Controlled Release, in press. <presented in Chapter 2 of this dissertation>

3. Gastrointestinal transit and mucoadhesive characteristics of complexation hydrogels in rats. Takahiro Goto, Mariko Morishita, Nikhil J. Kavimandan, Kozo Takayama, and Nicholas A. Peppas. Journal of Pharmaceutical Sciences, 95, 462-469 (2006). <presented in Chapter 3 of this dissertation>

4. Novel mucosal insulin delivery systems based on fusogenic liposomes. Takahiro Goto, Mariko Morishita, Ken Nishimura, Mahito Nakanishi, Atsushi Kato, Jumpei Ehara, and Kozo Takayama. Pharmaceutical Research, in press. <presented in Chapter 4 of this dissertation>

ABBREVIATIONS

AAC	area above the curve
ANOVA	analysis of variance
AUC	area under the insulin concentration-curve
BA	bioavailability
C_{max}	the plasma peak level
Chol	cholesterol
DMPA	dimethoxy propyl acetophenone
EDTA	ethylenediaminetetraacetic acid
EG	ethylene glycol
FL	fusogenic liposomes
F protein	fusion protein
GFP	green fluorescent protein
GI	gastrointestinal
GK rats	Goto-Kakizaki rats
HN protein	hemagglutinating and neuraminidase protein
IDE	insulin degrading enzyme
ILP	insulin-loaded polymer
Isc	short circuit current
LDH	lactate dehydrogenase
L-ILP	Large ILP
MAA	methacrylic acid
MRT	mean residence time
PA	pharmacological availability
PBS	phosphate-buffered saline
PC	phosphatidylcholine
PCMB	*p*-chloromercuribenzoate

PD	transmucosal potential difference
PEG	poly(ethylene glycol)
PEGMA	poly(ethylene glycol) monomethylether monomethacrylate
PG	phosphatidylglycerol
P(MAA-g-EG)	poly(methacrylic acid) grafted with poly(ethylene glycol)
Rm	membrane electrical resistance
SeV	Sendai virus
S-ILP	Small ILP
SS-ILP	Super-Small ILP
TEGDMA	tetraethylene glycol dimethacrylate
T_{max}	the time taken to reach the plasma peak level

GENERAL INTRODUCTION

Over the past several decades, biotechnology has developed extensively and led to a significant increase in the number of bioengineered products. The progress of these fields has had a great impact on the therapeutic agents used to treat many diseases, such as diabetes, etc., which are often difficult to treat with current medicines. Most of these products are peptides and proteins, which are generally administered via the parenteral route. However, oral administration is the most desirable route for taking these drugs because of ease of administration, thus resulting in good patient compliance.

Insulin remains the most effective drug for a diabetic patient to control their blood glucose levels. The route for insulin delivery is restricted to subcutaneous injections, as opposed to the oral route, due to insulin inactivation by proteolytic enzymes in the gastrointestinal (GI) tract and low permeability through the intestinal membrane [1,2]. However, the subcutaneous injection of insulin has various disadvantages such as hyperinsulinemia, pain, allergic reactions and low patient compliance. Another important issue with insulin is that parenteral administration does not replicate the normal dynamics of endogenous insulin release, resulting in a failure to achieve a lasting glycemic control in patients [3,4]. The portal delivery of insulin, which mimics endogenous insulin release, can be achieved via intestinal administration. Obviously, from this perspective, the development of an oral delivery system providing adequate bioavailability of insulin would revolutionize the treatment of diabetes. Moreover, it can be anticipated that such a technique could be applied to delivery of other protein drugs.

To date, various strategies have been developed to try and achieve an oral insulin

delivery system, including co-administration with absorption enhancers [5,6] or enzyme inhibitors [6,7], chemical modification [8], polymeric carriers [9-11], and lipid-based carriers as liposomes [12] and solid lipid nanoparticles [13]. Nevertheless, these approaches show low bioavailability and also some of them exhibit several negative effects such as irritation of the intestinal mucosal membrane and impairment of the membrane barrier. Therefore, it was essential to develop effective and reliable oral delivery systems for this class of drugs. For such a development to succeed, oral peptide and protein drug delivery systems should contain at least two essential requirements. First, the system should protect the drugs from enzymatic degradation. Second, the system should increase the drug permeability within the intestinal membrane. A formulation that satisfies these requirements is encapsulation or incorporation, which is the most widely used formulation strategy for peptide and protein delivery systems. To date, various carriers have been used to develop such drug delivery systems, however, the carriers have not shown sufficient bioavailability when administered by the oral route.

In Chapters 1~3, I discussed complexation hydrogel networks of poly(methacrylic acid) grafted with poly(ethylene glycol) (P(MAA-g-EG)) for oral insulin delivery systems. The P(MAA-g-EG) hydrogels were shown to exhibit pH-dependent swelling behavior due to the formation/dissociation of interpolymer complexes as shown in Fig.1 [14-16]. In the acidic environment of the stomach, these copolymers form interpolymer complex due to hydrogen bonding between etheric groups of the graft PEG chain and the acidic protons of the MAA network [14-16]. Under these conditions, the network mesh size is significantly decreased and diffusion of insulin through the network is prevented [14-16]. Hence, insulin loaded into the hydrogels

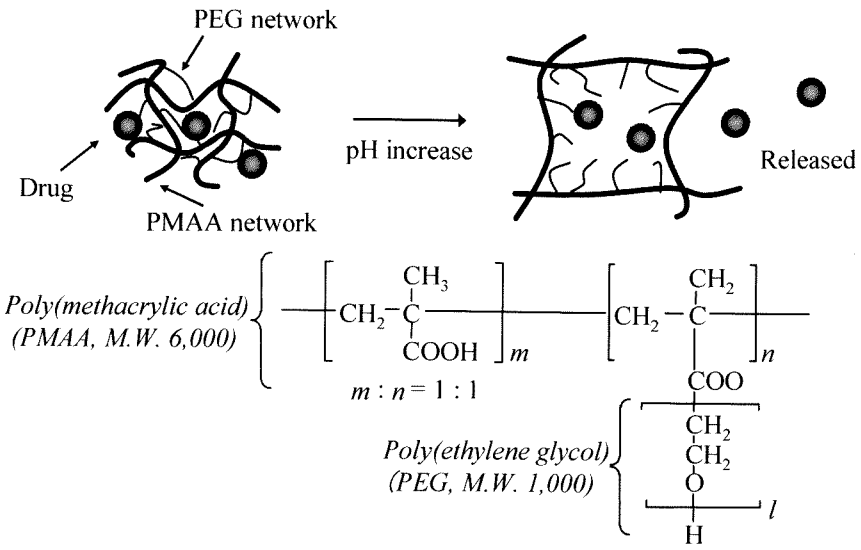

Fig. 1. Reversible interpolymer complexation / decomplexation of complexation polymer hydrogels

can be protected from proteolytic degradation by gastric enzymes such as pepsin. In the basic/neutral environment of the small intestine, the complexes immediately dissociate due to repulsion of ionized pendant acid groups and the network's pore size rapidly increases, leading to the release of insulin. The polymer is capable of highly incorporating and rapidly releasing insulin *in vitro* [17]. Furthermore, P(MAA-g-EG) has the ability to protect insulin from proteolytic degradation by inhibiting calcium dependent proteases such as trypsin and alpha-chymotrypsin [16] and the polymer shows mucoadhesive characteristics [18]. Insulin-loaded P(MAA-g-EG) microparticles (henceforth designated as ILP) (with a molar ratio of MAA:EG=1:1 and particle diameters of 100 to 150 μm) successfully enhanced oral insulin absorption in healthy and streptozotocin-induced type 1 diabetic rats, with up to 4.2 % bioavailability [19]. Nevertheless, further optimization of the polymer delivery system is required to improve clinical application. Therefore, in Chapters 1 and 2, I discussed to find an optimal formulation for oral insulin delivery in *in situ* and *in vivo* experiments, focusing on the particle size and polymer composition.

In Chapter 3, I focused on the mucoadhesive characteristics of complexation hydrogels. Mucoadhesion refers to adhesion between polymer carriers and the mucosa and is exhibited by certain polymers which become adhesive upon hydration. The goal of mucoadhesive drug delivery systems is to increase the residence time of therapeutic molecules at the specific sites within the GI tract for absorption of the drug into the circulation. It is believed that complexation hydrogels have excellent mucoadhesive characteristics because PEG tethers attached to the polymer network act as adhesion promoters [18,20]. However, the mucoadhesive characteristics of the P(MAA-g-EG) microparticles in the GI tract have not been studied *in vivo*. Fully understanding the mucoadhesive characteristics in the GI tract is of importance for therapeutic application.

In Chapter 4, I discussed novel drug delivery carrier, fusogenic liposomes (FL), to further improve the mucosal absorption of insulin. FL are prepared by fusing conventional liposomes with inactivated Sendai virus (SeV) particles, and can deliver encapsulated contents directly and efficiently into the cytoplasm through membrane fusion, with the same mechanism as SeV infection as shown in Fig. 2 [21-23]. The FL envelope glycoproteins, hemagglutinating and neuraminidase (HN) and fusion (F) protein, have critical roles in the process of membrane fusion [24]. The HN protein is involved in cell binding through attachment of the virus envelope to the cellular receptors containing sialic acid, while F protein plays a major role in fusion of the envelope with the cell membrane. So far, these SeV-mediated drug delivery systems have been used to successfully introduce many kinds of macromolecules, such as DNA, proteins, and nano-carriers, into animal cells [21-23]. However, the feasibility of applying this fusion-mediated delivery system to the intestinal mucosal membranes has

not yet been established.

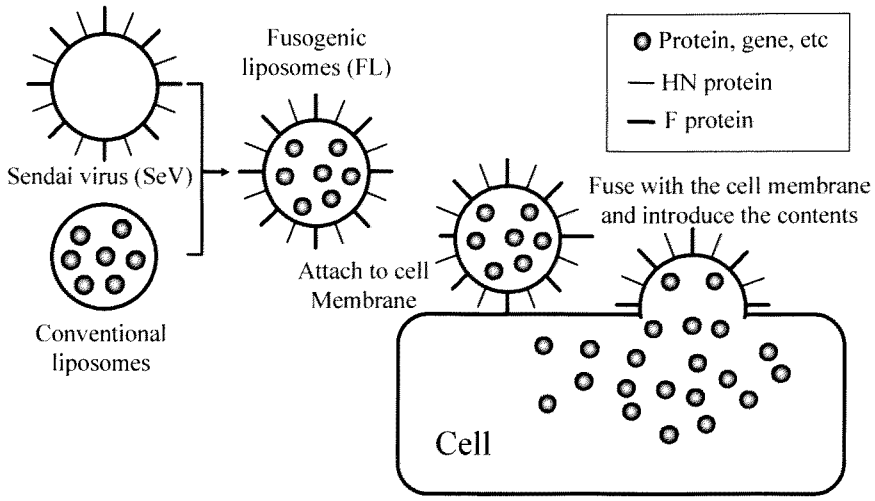

Fig. 2. The principle of fusogenic liposome-mediated macromolecular delivery

In Chapter 1, in order to further improve the oral bioavailability of insulin by ILP, the effect of particle size of the ILP on insulin absorption was studied in the *in situ* loop system. In addition, the safety of P(MAA-g-EG) microparticles as a carrier via the oral route was examined. Chapter 2 aimed to identify an optimal formulation and prove the excellent ability of the prepared particles for controlling blood glucose levels of diabetic rats via oral route in the *in vivo* experiments. In Chapter 3, the GI transit and mucoadhesive characteristics of complexation hydrogels was estimated. In Chapter 4, the potential of the FL to improve the mucosal absorption of insulin from rat intestinal membranes was evaluated in the *in situ* loop method.

Chapter 1

Mucosal insulin delivery systems based on complexation polymer hydrogels: effect of particle size on insulin enteral absorption

1. Introduction

A successful formulation for oral delivery of therapeutic peptide and protein drugs would have to overcome two main barriers against the drugs: the enzymatic barrier of the GI tract and the physical barrier made of the intestinal epithelium. In order to overcome these barriers, the multifunctional carrier system, complexation hydrogels showing high insulin incorporation efficiency, a rapid insulin release in the intestine based on their pH-dependent complexation properties, enzyme-inhibiting effects and mucoadhesive characteristics has been developed. Lowman et al. reported that the insulin incorporated into P(MAA-g-EG) microparticles (diameter 100-150 μm) successfully enhanced insulin oral absorption in both streptozotocin-induced diabetic and non-diabetic rats, achieving 4.2 % bioavailability (relative to subcutaneous administration) with significant hypoglycemic effects [19]. However, nevertheless, further improvement of the delivery system is required for their clinical application. If the size of P(MAA-g-EG) microparticles is decreased, the mucoadhesiveness would be increased due to an increase of surface area contact with the mucosa. If so, significant quantities insulin could be released closer to the surface of intestine, which might result in a decrease of protease attack and improved uptake of intact drug. Therefore, it was hypothesized that smaller particle sizes of the polymer carrier could induce greater hypoglycemic effects.

In this chapter, the effect of particle size of P(MAA-g-EG) on insulin absorption was studied in the *in situ* absorption system. The mucoadhesion on the mucosal tissues was compared among differently sized P(MAA-g-EG) microparticles to verify this hypothesis. Additionally, insulin release profiles from differently sized microparticles were evaluated. Furthermore, insulin absorption using the most effective

P(MAA-g-EG) microparticles were compared at various intestinal segments to determine their site-specific effects. Finally, to ensure the safety of P(MAA-g-EG) microparticles as a carrier via the oral route, intra- and inter-cellular integrity and/or damage were examined by lactate dehydrogenase (LDH) leakage and membrane electrical resistance (Rm) changes.

2. Experimental section

2.1. Materials

Methacrylic acid (MAA), dimethoxy propyl acetophenone (DMPA) and lactate dehydrogenase reagent were purchased from Sigma-Aldrich Co. (St. Louis, MO, USA). Poly(ethylene glycol) (PEG) monomethacrylate (PEGMA, with nominal PEG molecular weight of 1000, corresponding to 23 repeating units) and tetraethylene glycol dimethacrylate (TEGDMA) were obtained from Polysciences (Warrington, PA, USA). Crystalline human insulin (26.7 units/mg) was kindly supplied by Aventis Research and Technologies (Frankfurt, DE). All other chemicals were of analytical grade and commercially available.

2.2. Synthesis of complexation hydrogels

P(MAA-g-EG) microparticles were synthesized by a free-radical solution polymerization of MAA and PEGMA with PEG of molecular weight 1000. The monomers were mixed to yield solutions with a 1:1 ratio of MAA/EG in the gels. As a crosslinking agent, TEGDMA was added in the amount of 0.075 mol TEGDMA per mole MAA. Following the complete dissolution of the monomer, nitrogen was bubbled through the well-mixed solutions for 30 min to remove dissolved oxygen, a free radical scavenger, which would act as an inhibitor for polymerization. The initiator, DMPA, was added in the amount of 1 % weight of the monomers in a nitrogen atmosphere. The reaction mixtures were pipetted between flat plates to form films of 0.9 mm thickness. The monomer films were exposed to UV light (Ultracure 100, Efos, Buffalo, NY, USA) at 1 mW/cm^2 at 365 nm and allowed to react for 30 min. The ensuing hydrogels were rinsed for a week in deionized water to remove unreacted

monomer and uncrosslinked oligomer chains, then dried under vacuum and ground into powders with diameters of <43 (Super-small ILP; SS-ILP), 43–89 (Small ILP; S-ILP) and 180–230 (Large-ILP; L-ILP) μm.

2.3. Insulin incorporation

Insulin loading was performed by equilibrium partitioning in pH 7.4 phosphate-buffered saline (PBS) as described previously [17]. Briefly, specific amounts of crystalline human insulin were dissolved in 0.1 mL of 0.1 M HCl. The insulin solution was diluted with 19.8 mL of PBS and pH was adjusted to 7.4 with 0.1 mL of 0.1 M NaOH. Loading was accomplished by soaking 140 mg of each set of the dried P(MAA-g-EG) microparticles for 2 h in the insulin solution. The microparticles were collapsed with 20 mL of 0.1 M HCl and filtered using cellulose acetate/cellulose nitrate filter with 1 μm pores (Fisher Scientific International, Hanover Park, IL, USA). The insulin-loaded polymers (ILP) were dried under vacuum and stored at 4 ℃ until use. The amount of insulin into hydrogels was determined by HPLC. The HPLC was composed of a pump (LC-10AS, Shimadzu Co. Ltd., Kyoto, Japan), a UV detector (SPD-10A, Shimadzu), a system controller (SCL-10A), an auto injector (SIL-10A, Shimadzu), an integrator (C-R3A, Shimadzu) and a GL-PACK Nucleosil 100-5C18 column (150×4.6 mm i.d.). The mobile phase was a mixture of acetonitril:0.1 % trifluoroacetic acid:NaCl=31:69:0.58, v/v/w%. The flow rate was 1.0 mL/min and UV detection was performed at a wavelength of 220 nm. Insulin incorporation efficiency was unaffected by the size of ILP, and reached more than 90 % of the initial amount.

2.4. *In situ* absorption study

The animal experiments in this work complied with the regulations of the Committee on Ethics in the Care and Use of Laboratory Animals at Thomas Jefferson and Hoshi Universities. Male Sprague-Dawley rats weighing 180-200 g fasted for 24 h prior to the experiments and were anesthetized by an i.p. injection of 50 mg/kg sodium pentobarbital. The rats were restrained in a supine position and kept at body temperature of 37 °C using warming lamps. The jejunum, the ileum or the colon was exposed following small midline incision carefully made in the abdomen, and each segment (length=10 cm) was cannulated at both ends using polypropylene tubings (4 mm o.d., 2 mm i.d., Cole-Parmer Instrument, Vernon Hills, IL, USA). These were securely ligated to prevent fluid loss and subsequently, carefully returned to their original location inside the peritoneal cavity. In order to wash the intestinal content, phosphate-buffered saline (PBS; pH 7.4) at 37 °C were singly circulated through the cannula at 1.0 mL/min for 20 min using a peristaltic pump (MasterFlexR tubing pumps, Cole-Parmer Instrument). Subsequently, the segments were tightly closed following removal of cannulation tubings; approximately 0.5 mL of perfusion solutions remained left in the segments. Rats were further left on the board at 37 °C for 1 h to be recovered from the elevated blood glucose levels due to surgical operations described above. Following 1 h resting, pure insulin or each ILP (approximately 3 mg) with 0.5 mL of PBS solution was directly administered into the loops (6 cm) made from the pretreated segment (10 cm); the jejunal loop was made at 5 cm away from the ligament of Treitz; the ileal loop was made at the end of the small intestine, just proximal to the ileo-cecal junction; the colonic loop was made at the ascending colon. Insulin PBS solution (0.5 mL) was used as a control. The dose for all samples was fixed at 25 IU/kg body weight. During the experiment, a 0.2 mL blood aliquot was taken from the

jugular vein at t = 0, 5, 10, 15, 30, 60, 120, 180 and 240 min after dosing. The relative bioavailability of the enterally administered insulin was calculated relative to the subcutaneous (s.c.) route, using methods described by Matsuzawa et al. [25]. Briefly, insulin solutions were prepared by dissolving an appropriate amount of crystalline human insulin in PBS. The insulin s.c. doses were 0.25, 0.5, 1.0 and 2.0 IU/kg body weight. Blood samples (0.2 mL) were collected from jugular vein before and 5, 10, 15, 30, 60, 120, 180 and 240 min after dosing. Animals receiving s.c. insulin were given the same surgical operation (the ileal loop) as in the intestinal administration study, in order to set the same physical condition on the rats. Tuberculin syringes (1 mL) were pre-heparinized in the usual fashion consisting of coating of the syringe wall through aspiration of heparin and expelling all heparin by depressing plunger down to needle hub. Plasma was separated by centrifugation at 13,000 rpm for 1 min. The plasma glucose levels were determined using HemoCueR B-glucose analyzer (HemoCue, CA, USA). The plasma insulin levels were determined using an enzyme immunoassay (Alpco Research, Windham, NH, USA). The total area under the insulin concentration curve (AUC) from time 0 to 240 min was estimated from the sum of successive trapezoids between each data point. The bioavailability was calculated relative to s.c. injection as described above. The plasma peak level (C_{max}) and the time taken to reach the plasma peak level (T_{max}) were determined from the plasma insulin level–time curves. Mean residence time (MRT) was calculated by dividing AUMC by AUC, where AUMC is the area under the first moment curve for insulin from 0 to 240 min point.

2.5. *In vitro* release study

The formulations (10 mg) were placed into beakers containing 20 mL of PBS at 37

°C under constant stirring. Samples (0.1 mL) were taken at discrete intervals using filtered syringes (pore size: 10 μm; Ishikawa Manufactory). Insulin concentration in each sample was determined by using HPLC method described above. The fractional release of insulin from the formulations, defined here as the ratio of the amount released at any time (M_t) to the total amount released after 1 h (M_1) was calculated.

2.6. Mucoadhesion study

The jejunal and the ileal loops from the pretreated segment following the *in situ* experiments as described above were used. Following washing of the remaining PBS in the loop with air, L-ILP or SS-ILP (each 30 mg) with 0.5 mL of PBS was administered to each loop and remained in the segments for 1 h. Then, the loops were washed by circulating PBS at 1.0 mL/min for 1 min using a peristaltic pump. The detached microparticles were collected, dried under vacuum and weighed. The mucoadhesive capacity (%) was calculated as (the initial amount (30 mg) - the collected amount) × 100/the initial amount (30 mg)).

2.7. Biochemical evaluation of intestinal damage

The ileal loop from the pretreated segment following the *in situ* experiments as described above was used here. The ileum was treated with 20 mL of PBS (warmed to 37 °C) and then flushed out with air. One milliliter of PBS, 1 % (w/v) sodium caprate, 1 % (w/v) sodium glycocholate or SS-ILP (5 mg) PBS suspension was administered to the ileum and incubated in the segments for 2 h. Then, the ileal loop was washed with 1.0 mL of PBS, and the intestinal fluid was collected. The concentration of lactate dehydrogenase (LDH) in the fluid was determined using a LDH-UV kit (Sigma-Aldrich

Co., St. Louis, MO, USA).

2.8. Ileal membrane electrical resistance

The ileal loop from the pretreated segment following the *in situ* experiments as described above was used in this experiment. Following washing the ileum with warmed 20 mL of PBS, the remaining PBS in the loop was then washed out with air. Then, 10 mg of SS-ILP with 0.5 mL of PBS was administered to the ileal loop and remained left for 5 and 30 min. Similarly, 0.5 mL of control (PBS) or 20 mM Na_2EDTA (ethylenediaminetetraacetic acid), as a positive control, was administered to the ileal loop for 5 and 30 min. Immediately after each pretreatment, the ileal segments were quickly opened along the mesenteric border to prepare the flat sheet membranes. They were carefully washed with ice-cold calcium free Krebs–Ringer's bicarbonate-buffered solution (pH 7.4) [26]. The solution (in mM) was composed of 125.0 NaCl, 11.1 D-glucose, 10.0 $NaHCO_3$, 5.0 KCl, 1.2 NaH_2PO_4, and 4.2 mannitol. The membranes were mounted in an Ussing chamber system (CEZ-9100, Nihon-Kohden Tokyo, Tokyo, Japan) equipped with diffusion cells of 1 cm^2 as the effective area maintained at 37 °C. Apical and basal compartments were filled with 5.0 mL of isotonic calcium free Krebs–Ringer's solution and stirred with oxygenation (95 % O_2/5 % CO_2) for 20 min prior to monitoring electrophysiological parameters. The spontaneous transmucosal potential difference (PD, mV) and the short circuit current (Isc, AA) were recorded simultaneously at 20 min, and Rm (V) calculated by PD/Isc, based on the Ohm's law. These were corrected by eliminating the offset voltage between the electrodes and series fluid resistance, which was determined prior to each experiment using the identical bathing solutions, yet in the absence of ileal

membranes mounted in the chamber.

2.9. Statistical analysis

The results were expressed as the mean ± S.D. For group comparison, an analysis of variance (ANOVA) with a one-way layout was applied. Significant differences in the mean values were evaluated using Student's t-test. Differences were considered to be significant when the p value was less than 0.05.

3. Results

3.1. Effect of particle size of ILP on insulin absorption from the ileum

Figure 3 shows the effect of particle size of ILP on insulin absorption (A) and resultant hypoglycemic effect (B). No apparent hypoglycemic response was observed in the control group, demonstrating no insulin absorption from the ileal segments. Similarly, L-ILP demonstrated the absence of appreciable insulin absorption from the ileal segments although plasma glucose levels seemed to be lower than those of control. In contrast, S- and SS-ILP significantly enhanced insulin ileal absorption. SS-ILP showed more predominant enhancement effect on insulin absorption than that of S-ILP, implying that the smaller size of ILP induced the bigger insulin absorption from the ileum.

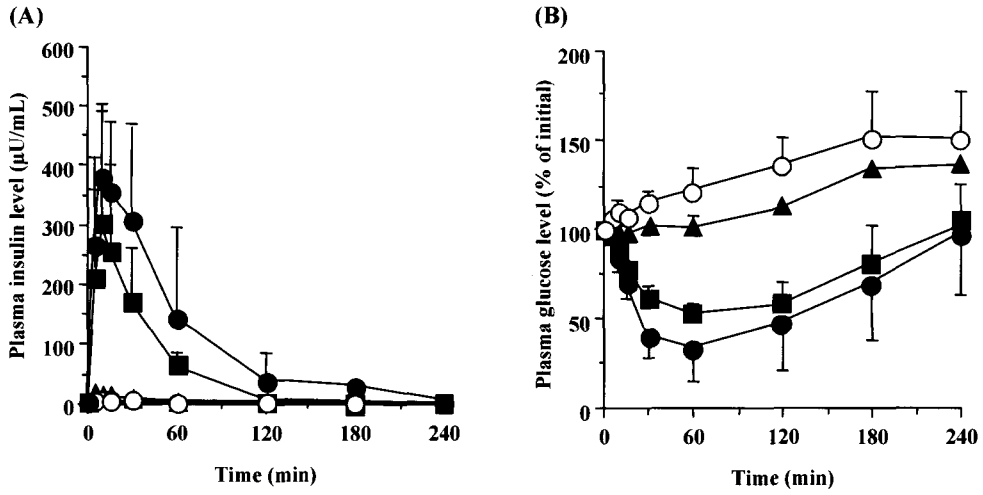

Fig. 3. Plasma insulin (A) and plasma glucose (B) level versus time profiles following *in situ* administration of ILP (25 IU/kg) into the ileal segments. Each data represents the mean ± S.D. (n=3-4). Key: (open circle) insulin PBS solution (control); (closed triangle) L-ILP; (closed square) S-ILP; (closed circle) SS-ILP.

Table 1 summarizes pharmacokinetic parameters derived from the insulin concentration–time profiles following *in situ* administration of ILPs to the ileal segments. In this study, the relative bioavailability of insulin was calculated based on

the s.c. injection study (Fig. 4). Plotting AUC of insulin vs. dose, there is the linear relationship having r= 0.934 (n=17, $p<0.01$). While there is no significant difference in pharmacokinetic parameters between control and L-ILP, S- and SS-ILP induced the significant increase in parameters, C_{max}, AUC and BA, which are related to the extent of absorption. On the other hand, T_{max} and MRT appeared to be unaffected by the reduction of the size of ILP.

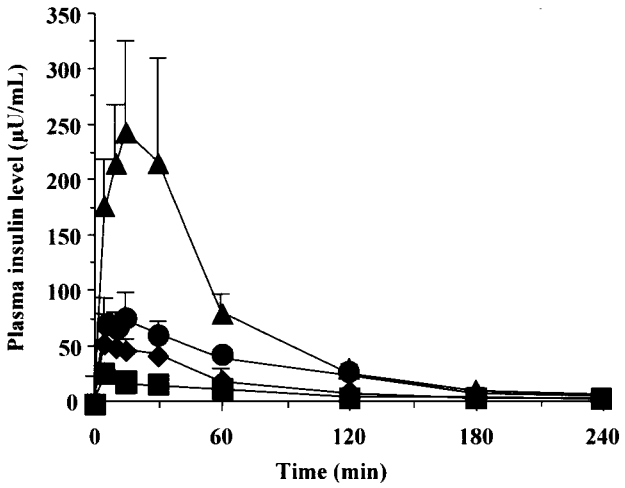

Fig. 4. Plasma insulin level versus time profiles following s.c. administration of insulin solution. Each data represents the mean ± S.D. (n=4). Key: (closed square) 0.25 IU/kg; (closed diamond) 0.5 IU/kg; (closed circle) 1.0 IU/kg; (closed triangle) 2.0 IU/kg.

Table 1.

Pharmacokinetic parameters derived from the plasma level vs. time profiles for insulin (25 IU/kg), following *in situ* administration into ileal segments

Preparation	C_{max} (μU/mL)	T_{max} (h)	MRT (h)	AUC (μU ·h/mL)	BA (%)
Control	3.9 ± 4.4	0.20 ± 0.39	0.38 ± 4.60	2.5 ± 3.3	0.5 ± 0.1
L-ILP	7.8 ± 7.9	0.17 ± 0.28	0.48 ± 0.41	6.1 ± 7.2	0.7 ± 0.2
S-ILP	299.7 ± 202.5 *	0.08 ± 0.12	0.35 ± 0.20	149.4 ± 90.5 *	5.2 ± 2.8 *
SS-ILP	411.6 ± 82.0 *	0.14 ± 0.24	0.76 ± 0.21	391.4 ± 263.7 *	12.8 ± 8.3 *

Each data represents the mean ± S.D. (n=3-4).

C_{max}: the plasma peak level; T_{max}: the time taken to reach the plasma peak level; AUC: the area under the curve; BA: Relative bioavailability compared to s.c.

Significant difference from the control: $p<0.05$, *.

3.2. Effect of particle size of ILP on insulin release profiles

Figure 5 shows the effect of particle size of ILP on insulin release profiles. It should be noted that these curves represent the release behavior of insulin from ILPs in PBS because insulin was not released from ILPs in acidic condition. As shown in Fig.5, each ILP can release insulin in the neutral condition. In addition, insulin was far more rapidly released from SS-ILP than that from L-ILP in neutral condition.

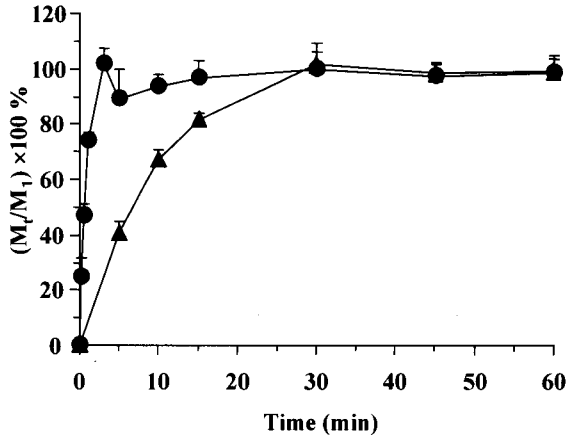

Fig. 5. Release profiles of insulin from P(MAA-g-EG) microparticles. Each data represents the mean ± S.D. (n=3-6). Key: (closed triangle) L-ILP; (closed circle) SS-ILP.

3.3. Effect of particle size of ILP on its adhesive capacity to the mucosal tissues

Figure 6 shows the effect of particle size of P(MAA-g-EG) on the mucoadhesive characteristics to the jejunal and ileal mucosa. It was demonstrated that more than 60 % of administered SS-ILP microparticles were tightly adhered to both the jejunum and the ileum tissues following 1 h administration. Likewise, L-ILP showed a high mucoadhesive capacity at both intestinal regions, however, the values were significantly lower than those of SS-ILP. Similar trends were observed following 5 min administration (data not shown).

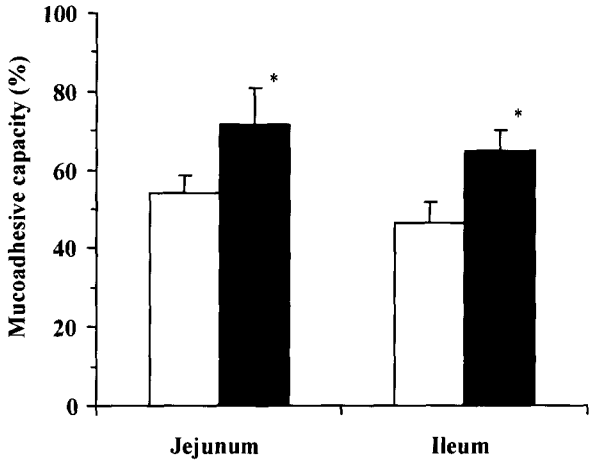

Fig. 6. Mucoadhesive capacities of P(MAA-g-EG) microparticles at jejunal and the ileal regions. Each data represents the mean ± S.D. (n=3). Key: (open column) L-ILP; (closed column) SS-ILP. Statistically significant difference from L-ILP: $p < 0.05$, *.

3.4. Comparison of hypoglycemic effects following administration of SS-ILP to various intestinal segments

Figure 7 shows the insulin absorption following SS-ILP administration into the ileal, the colonic, and the rectal segments. The hypoglycemic effects induced by SS-ILP were different at three intestinal regions. In the jejunal and colonic segments, relatively weak hypoglycemic effects were observed following SS-ILP administration, while SS-ILP induced the dramatic reduction of blood glucose levels in the ileal segment.

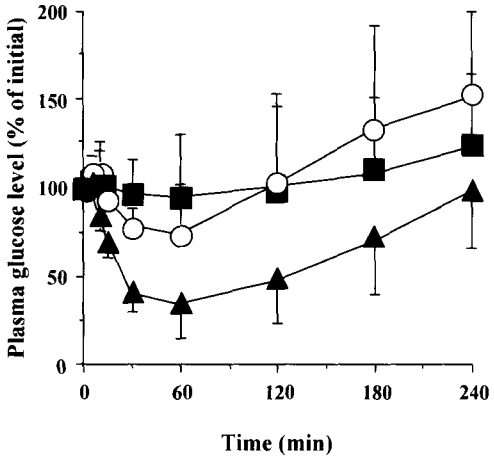

Fig. 7. Blood glucose level versus time profiles following *in situ* administration of SS-ILP (25 IU/kg) into various site of intestine. Each data represents the mean ± S.D. (n=4-5). Key: (open circle) jejunum; (closed triangle) ileum; (closed square) colon.

3.5. Biochemical and electrophysiological characterization of the ileal membranes following SS-ILP administration

Table 2 shows the LDH leakage following 2 h administration of SS-ILP to the ileal region. Lactate dehydrogenase was negligibly leaked into the ileal loop, which was similar to the leakage seen in the control group. In contrast, the leakage was dramatically induced by administration of typical penetration enhancers, 1.0 % (w/v) sodium caprate and 1.0 % (w/v) sodium glycocholate. Likewise, the values for Rm were unchanged following application of SS-ILP to the ileal region, compared to those in the PBS-treated (control) counterparts (Table 3). This was quite contrastive to active control, Na_2EDTA-treated segment which induced significant decrease in the values of Rm. These data suggested that the ileal membrane integrity and cellular tight junctions remain mostly unaltered by the administration of SS-ILP.

Table 2.

Lactate dehydrogenase (LDH) leakage following application of PBS (control), SS-ILP, 1.0% (w/v) sodium caprate and 1.0% (w/v) sodium glycocholate

Preparation	LDH leakage (U)
Control	0.39 ± 0.17
SS-ILP	0.47 ± 0.11
Sodium caprate	1.13 ± 0.39 *
Sodium glycocholate	2.35 ± 1.19 **

Each value represents the mean ± S.D. (n=4-6).

Statistically significant difference from control: $p<0.01$,**; $p<0.05$,*.

Table 3.

Membrane electrical resistance (Rm) following application of PBS (control), SS-ILP and Na_2EDTA into the ileal segment

Preparation	Rm ($\Omega \cdot cm^2$)	
	5 min	30 min
Control	42.7 ± 5.0	42.3 ± 2.9
SS-ILP	40.2 ± 4.3	36.1 ± 2.0
Na_2EDTA	24.6 ± 5.2 *	25.4 ± 2.9 *

Each value represents the mean ± S.D. (n=3-4).

Statistically significant difference from control: $p<0.05$,*.

4. Discussion

The copolymer hydrogel networks of poly(methacrylic acid) grafted with poly(ethylene glycol) (P(MAA-g-EG)) is a promising class for oral carriers of insulin [14-19]. Nevertheless, further optimization of the polymer delivery system is required to improve clinical application. One of the important factors for improving insulin absorption from the small intestine may be the particle size of ILP. Smaller size of ILP would induce bigger hypoglycemic effects due to increased mucoadhesive capacity to the intestinal mucosa. Therefore, the effect of particle size of ILP on the enteral insulin absorption was investigated in the *in situ* loop system.

As shown in Fig. 3, a reduction of particle size of ILP significantly increased the hypoglycemic effect, with the diameters of <43 μm (SS-ILP) showing the highest BA values (Table 1). These results suggest that the particle size of the hydrogels play a critical role in oral insulin delivery. One of important factors is the enhancement effect of mucoadhesion of the hydrogels. P(MAA-g-EG) exhibits excellent mucoadhesive characteristics for delivery of drugs to the small intestine due to the presence of the graft PEG chains which serve as adhesion promoters [18,20]. Thus, a size-dependent particle deposition in the GI tract of rats has been suggested recently [28,29]. The authors report that small size microparticles easily interpenetrate into the mucus layers and increase mucoadhesive characteristics to the intestinal mucosa. The similar phenomenon was observed in Fig. 6. The SS-ILP showed higher mucoadhesive capacities to the intestinal mucosa than L-ILP. These results can support our hypothesis that the smaller size of ILP may give the stronger bioadhesive competence. In addition, particle size also affected insulin release profiles in the neutral condition, and insulin was more rapidly released from the smaller size microparticles (Fig. 5).

These imply that the smaller particle size can provide for near instant insulin release at the absorption site resulting in closer insulin release to the membrane epithelium and, thereby, in an increase of the number of insulin molecules those can escape from proteolysis in the lumen and more amount of insulin can be absorbed.

Generally, when insulin solutions are administered to the small intestine, insulin is subjected to extensive degradation by proteolytic enzymes and, thereby, insulin absorption occurs negligibly like control group of this study. It has been shown that insulin is degraded by pancreatic proteases like trypsin and chymotrypsin, which are believed to reside in both intestinal fluids and the mucus/glycocalyx layers [1,2]. In this study, enzymes in the former compartment could be removed by washing pretreatment with PBS in the *in situ* experiments. However, the mucus/glycocalyx layers might remain and in fact, the layers have significant roles in insulin's metabolic loss [1,2]. Moreover, the importance of ectopeptidases contributing to the metabolic loss of certain polypeptides including insulin has been reported [30,31]. Regardless of such multi-compartment enzymatic barriers, however, the ileal insulin absorption clearly occurred in the small intestine following the application of S- and SS-ILP. One possibility of the increased insulin's absorption may be associated with the reduced proteolytic activity in the presence of the polymer. It has been already reported that P(MAA-g-EG) microparticles may inhibit the metal-dependent enzymes via the binding of Ca^{2+} with carboxylic group on the backbone chain [16]. Indeed, a range of proteases can be inhibited by chelating essential metal ions from the enzyme structure, resulting in protein denaturation and loss of activity [32]. Therefore, this may play the crucial role for the enhancing absorption of insulin following ILP administration.

The SS-ILP's enhancement effect of insulin mucosal absorption showed a

site-specificity, demonstrating maximum effect at the ileal segment (Fig.7). The possible explanation of the results is due to the difference in proteolytic activity in the intestine. Comparing the pancreatic enzyme activity, it was much stronger in the upper small intestine than in the descending small intestine like the ileal segments [33]. Assuming that amount of released insulin from SS-ILP at each region would be the same, indeed, pH value in the intestinal fluid is thought to be enough for SS-ILP swelling, the degree of insulin degradation was much larger in the jejunum than in the ileum. As a consequence, the net insulin amount capable of being absorbed through the small intestine is much smaller in the jejunum than in the ileum and, therefore, it was likely that SS-ILP administration to the jejunal segment revealed small hypoglycemic effect. On the other hand, SS-ILP administration to the colonic segment, where the proteolytic activity may be much smaller than those in the small intestine, induced little or no hypoglycemic effects. The result is presumably due to the thickness of mucus layers [34] and tightness of tight junctions of the colon [35]. It is well known that the presence of the mucus layers was one of the permeation barriers for peptide and protein drug absorption [36–38]. It was demonstrated that the diminishment of mucus/glycocalyx layers showed the significant increase of insulin permeability [1,2]. Furthermore, the tight junction is more rigid in the large intestine than in the small intestine, so the permeability of macromolecular drugs from the large intestine might be lowered compared with the small intestine [35]. Although PEG chain grafted in PMAA was penetrated into mucus layers [18,20], and P(MAA-g-EG) may be adhered to the mucosal membrane, because of having thicker mucus layers and tightness of mucosal membrane in the colonic region, insulin absorption in the colon may be decreased, even though the insulin was released to the same extent in the

colonic segment as in the small intestine. These results suggest the necessity for oral P(MAA-g-EG) microparticles to be delivered into the lower small intestine to attain higher insulin absorption.

5. Conclusions

Smaller sized P(MAA-g-EG) microparticles (SS-ILP) showed the higher insulin absorption compared with the microparticles having larger size (L-ILP), resulting in greater hypoglycemic effects without detectable mucosal damage such as LDH leakage and Rm reduction. Furthermore, SS-ILP demonstrated higher mucoadhesive capacity to the jejunum and the ileum than those of L-ILP. The high mucoadhesive capacity may reduce insulin degradation in the mucus/glycocalyx layers, thereby increasing insulin absorption from the small intestine. A rapid burst-type release of insulin was observed with the smaller sized ILP which was believed to have contributed to an increased relative bioavailability of insulin. Moreover, SS-ILP's enhancement effect of insulin mucosal absorption showed a site-specificity, demonstrating maximum effect at the ileal segment. These results imply that the use of smaller size of P(MAA-g-EG) microparticles, and the delivery of them to the lower small intestine holds promise for increasing the bioavailability of insulin following oral administration.

Chapter 2

Oral insulin delivery systems based on complexation polymer hydrogels: Single and multiple administration studies in type 1 and 2 diabetic rats

1. Introduction

As shown in Chapter 1, ILP enhanced enteral insulin absorption with significant hypoglycemic effects without detectable mucosal damage. Recent *in vitro* studies suggest that the molar ratio of MAA:EG is an important parameter as it affects the insulin release behavior from microparticles, the ability of the carrier to protect insulin from enzymes, and the adhesive characteristics on the mucus membrane [17]. In addition, *in situ* absorption study described in Chapter 1 showed that the ILP particle size influenced strongly the intestinal insulin absorption with the smaller ILP size greatly enhancing insulin absorption, leading to a 12.8 % relative bioavailability. Based on observations obtained from the *in vitro* and *in situ* experiments, this chapter aimed to identify an optimal formulation and prove the ability of the prepared particles to act as carriers for oral insulin delivery in *in vivo* experiments. The most promising formulation would be used for *in vivo* single and multiple oral administration studies using type 1 and 2 diabetic rats.

2. Experimental section

2.1 Materials

MAA, DMPA, TEGDMA, and PEGMA were the same as described in Materials of Chapter 1. Streptozotocin was obtained from Sigma-Aldrich Co. (St. Louis, MO, USA). Crystalline recombinant human insulin (26.0 units/mg) was obtained from Wako Pure Chemical Industries Co., Ltd (Osaka, Japan). All other chemicals were of reagent grade and were used without further purification.

2.2 Synthesis of complexation hydrogels

Complexation hydrogels were synthesized by the same method as described in Synthesis of complexation hydrogels of Chapter 1. In this chapter, we prepared three different molar ratio of complexation hydrogels with 1:0, 4:1 and 1:1 MAA:EG units. In addition, particles size was adjusted with diameters of <53 (SS size) and 212-300 (L size) μm.

2.3 Insulin incorporation

Insulin incorporation was the same as described in Insulin incorporation of Chapter 1.

2.4 *In vivo* absorption study

This research complied with the regulations of the Committee on Ethics in the Care and Use of Laboratory Animals of Hoshi University. Male Wistar rats (180-200 g) were purchased from Sankyo Lab Service Co., Ltd. (Tokyo, Japan). Animals were housed in rooms controlled at 23±1 °C and 55±5 % relative humidity and allowed free access to water and food during acclimatization. Type 1 diabetes was induced by

intravenous injection of streptozotocin (55 mg/kg body weight) dissolved in a citrate buffer at pH 4.5. Three days after strepotozotocin treatment, the rats with a fasted blood glucose level >250 mg/dL were selected as type 1 diabetic rats. As a spontaneous model for type 2 diabetes [39], Goto-Kakizaki (GK) rats were used because GK rats display malfunctional insulin secretion against glucose and mild hyperglycaemia. GK rats were purchased from Sankyo Lab Service Co., Ltd. (Tokyo, Japan). The average pre-dose blood glucose levels of the healthy, type 1 and type 2 diabetic rats used in this study were 99±2, 319±6 and 149±4 mg/dL (mean ± SD, n=25-45), respectively. During the experimental period, rats were housed in cages and given water ad libutum. Rats were restrained in a supine position on a board during administration and blood sampling. Gelatin capsules (Qualicaps® capsule, Shionogi Quolicaps Co., Ltd, Nara, Japan) containing ILP (approximately 1, 3, and 6 mg at the insulin doses 10, 25, and 50 IU/kg, respectively) or insulin solutions were orally administered using a sonde needle.

In a single administration study in healthy rats, the insulin doses were 10, 25, and 50 IU/kg. In the case of type 1 and 2 diabetic rats, one insulin dose of 25 IU/kg was used. In order to calculate the efficacy of oral insulin administration relative to subcutaneous insulin, insulin solutions (1.0 IU/kg) were administered subcutaneously to healthy rats. Insulin solutions were prepared by dissolving an appropriate amount of crystalline human insulin in PBS. Rats were fasted for 48 h prior to the experiment. During the experiment, a 0.2 mL aliquot of blood was collected from the jugular vein at 0.25, 0.5, 1, 2, 4, 6, and 8 h following dosing.

In the multiple administration study, type 1 and 2 diabetic rats were fasted for 12 h prior to the study, and administered ILPs 3 times /day. Each insulin dose was fixed at

25 IU/kg. In the case of the multiple administration study, ILP (25 IU/kg) was also administered in combination with subcutaneous insulin (0.1 IU/kg), but only at the first dosing. The diabetic rats were fed for 30 min, 30 min after each drug administration and allowed free access to water. The hypoglycemic effects of SS-ILP were influenced by the fasting period of rats. Although the hypoglycemic effects were decreased by shortening the fasting period, sufficient insulin's effects were observed following oral administration of SS-ILP to the non-fasted rats (data not shown). These results suggest that SS-ILP may have the ability to reduce the blood glucose levels sufficiently under a feeding condition. In this study, therefore, the diabetic rats were fed for 30 min after each drug administration in the multiple oral administration study.

After blood sampling, the plasma was separated by centrifugation at 13,000 rpm for 1 min and kept at 4 °C until insulin concentration analysis. The plasma insulin concentrations were determined on the same day as the absorption study by an immuno-chemiluminometric assay (MLT research limited, Wales, UK) using a microplate luminometer (Mithras LB940, Beltold Japan Co., Ltd., Osaka, Japan). Blood glucose levels were determined using a glucose meter (Novo Assist Plus, Novo Nordisk Pharma Ltd., Tokyo, Japan). Post-dose blood glucose levels were expressed as a percentage of pre-dose blood glucose levels.

The extent of hypoglycemic response was calculated as the area above the blood glucose level-time curve below the 100 % line ($[AAC]_{p.o.}$ and $[AAC]_{s.c.}$ (% glu.reduc.·h) for oral and subcutaneous insulin to healthy rats, respectively) for 0-8 h. The relative pharmacological availability (PA(%)) of the orally administered insulin was calculated according to Eq. (1) in which $[AAC]_{s.c.}$ was determined after subcutaneous administration of 1.0 IU/kg of insulin.

$$PA(\%) = ([AAC]_{p.o.}/dose_{p.o.}) \times 100/([AAC]_{s.c.}/dose_{s.c.}) \quad (1)$$

2.5 Statistical analysis

The results were expressed as the mean ± SE. For group comparison, an analysis of variance (ANOVA) with a one-way layout was applied. Significant differences in mean values were evaluated by a Student's t-test. A difference was considered to be statistically significant when the *p* value was less than 0.05.

3. Results

3.1 Influence of the MAA/EG molar composition of the carrier hydrogel on oral insulin absorption

Figure 8 shows the blood glucose levels versus time profiles following oral administration of ILPs (<53 μm) with different molar ratios of EG to MAA at an insulin dose of 25 IU/kg to healthy rats. First, it is clear that no hypoglycemic effect was observed during administration of pure insulin solution, demonstrating the well known absence of insulin absorption via the oral route in the absence of a suitable carrier. Rather, blood glucose levels rapidly increased due to the physical stress during oral administration and blood sampling. Over the course of the study period, blood glucose levels did not return to the initial levels. However, the oral administration of insulin loaded microparticles prepared with a 1:1 molar ratio of MAA/EG units suppressed the initial rise in blood glucose levels as compared with other formulations. In addition, the blood glucose levels of the rats decreased remarkably, achieving a maximum hypoglycemic effect at 4 h, and with effects continuing up to 8 h. In the case of the microparticles prepared from 4:1 and 1:0 molar ratios of MAA/EG, a stress-induced increase in blood glucose levels occurred, as with the insulin solution, and there were no significant differences in blood glucose level-time profiles between control and both microparticle groups.

Figure 9 shows insulin and blood glucose level-time profiles following subcutaneous injection of an insulin solution to healthy rats at a dose of 1.0 IU/kg. Table 4 shows the values of the hypoglycemic response, the AAC, and the PA of each formulation calculated from the comparison of the AAC values to that of s.c. injection. The AAC values of insulin s.c. injection at a dose of 1.0 IU/kg was 57.6±9.5 %

glu.reduc. · h. While there is no significant improvement of the values of PA in the *in vivo* studies with administration of pure insulin solution, or insulin-loaded microparticles prepared from 1:0 and 4:1 molar ratios of MAA/EG, a remarkably higher PA was observed when using formulations based on ILPs with a 1:1 molar ratio of MAA/EG.

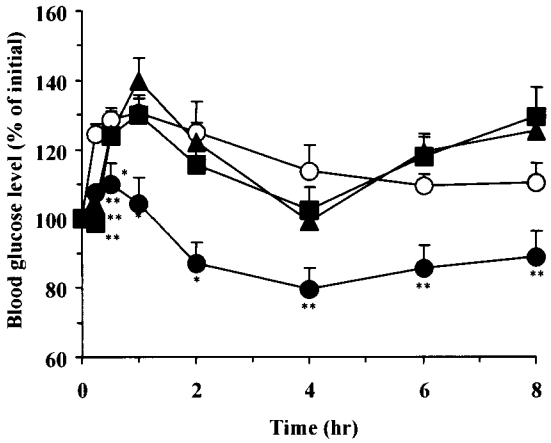

Fig. 8. Changes in blood glucose level versus time profiles following oral administration of ILP (25 IU/kg) containing different ratios of MAA:EG in healthy male Wistar rats. Each value represents the mean ± S.E. (n=6-12). Statistically significant difference from control: $p<0.01$,**; $p<0.05$,*. Key: (open circle) insulin solution (control); (closed square) MAA:EG=1:0; (closed triangle) 4:1; (closed circle) 1:1.

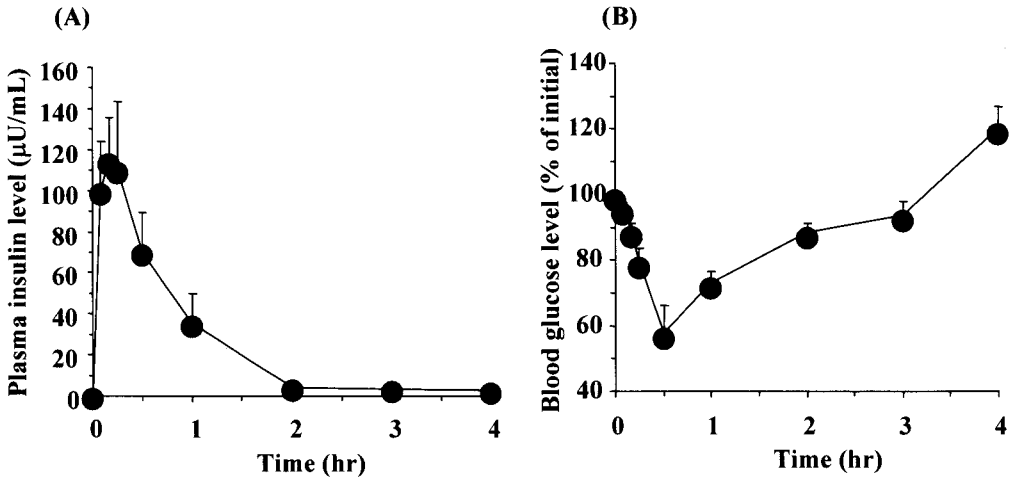

Fig. 9. Plasma insulin (A) and blood glucose (B) level versus time profiles in healthy male Wistar rats following subcutaneous injection of insulin solution (1.0 IU/kg). Each value represents the mean ± S.E. (n=3).

Table 4.

Pharmacological availability of insulin solution and various ILPs administered orally to Wistar rats

Preparation	AAC (% glu. reduc. · h)	PA (%)
Insulin solution	1.3 ± 0.8	0.0 ± 0.0
P(MAA-g-EG) microparticle		
MAA:EG=1:0	2.8 ± 1.7	0.2 ± 0.1
MAA:EG=4:1	2.5 ± 1.9	0.2 ± 0.1
MAA:EG=1:1	106.1 ± 47.3 **	7.4 ± 3.3 **

[a] AAC denotes area above the curve.

[b] PA denotes pharmacological availability.

Each value represents the mean ± S.E.

Statistically significant difference from insulin solution: $p<0.01$, **.

3.2 Influence of ILP particle size on oral insulin absorption

Figure 10 shows the insulin and blood glucose level profiles following oral administration of the 1:1 molar ratio of MAA/EG microparticles with diameters of <53 (SS-ILP) and 212-300 (L-ILP) μm and with an insulin dose of 25 IU/kg. The L-ILP samples did not induce any hypoglycemic effects and their profiles were close to those observed in the control group. In contrast, the SS-ILP induced insulin absorption from the GI tract, and resulted in significant hypoglycemic effects. This observation was consistent with the results of Chapter 1.

A dose-dependent insulin study was performed and the PA values following oral administration of ILPs at doses of 10, 25 and 50 IU/kg are summarized in Table 5. No pharmacological responses were observed following administration of an insulin solution even at the highest dose, 50 IU/kg. On the other hand, the ILPs exhibited higher PA values. Although the PA values of ILPs decreased as insulin doses increased,

the PA values were greater in SS-ILPs than L-ILPs at all insulin doses. Therefore, the SS-ILP formulation was selected as the most promising one and used for the in vivo single and multiple administration studies using diabetic rats.

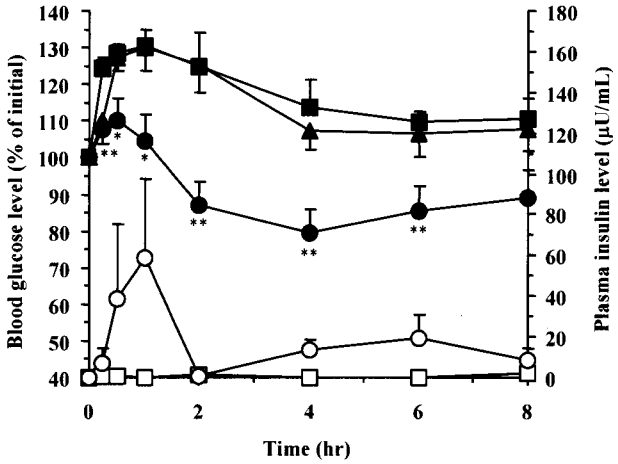

Fig. 10. Changes in plasma insulin (open symbol) and blood glucose level (closed symbol) versus time profiles following oral administration of different particle size of ILP (25 IU/kg) in healthy male Wistar rats. Each value represents the mean ± S.E. (n=6-12). Statistically significant difference from control: $p<0.01$,**; $p<0.05$,*. Key: (square) insulin solution (control); (triangle) L-ILP; (circle) SS-ILP.

Table 5.

Pharmacological availability of insulin solution and various ILPs administered orally to Wistar rats

Dose (IU/kg)	Preparation	AAC (% glu. reduc. · h)		PA (%)	
10	Insulin solution	0.7 ± 0.6		0.0 ± 0.0	
	L-ILP	19.0 ± 16.6	**	3.3 ± 2.9	**
	SS-ILP	54.6 ± 11.6	*	9.5 ± 2.0	*
25	Insulin solution	1.3 ± 0.8		0.0 ± 0.0	
	L-ILP	4.7 ± 3.2	**	0.3 ± 0.2	**
	SS-ILP	106.1 ± 47.3	*	7.4 ± 3.3	*
50	Insulin solution	1.7 ± 1.2		0.0 ± 0.0	
	L-ILP	14.3 ± 9.9	**	0.5 ± 0.3	**
	SS-ILP	51.5 ± 10.3	*	1.8 ± 0.3	*

[a] AAC denotes area above the curve.

[b] PA denotes pharmacological availability

Each value represents the mean ± S.E.

Statistically significant difference between the preparation: $p<0.01$, **; $p<0.05$, *.

3.3 Hypoglycemic effects following the single oral administration of SS-ILP to diabetic rats

Figure 11 shows the hypoglycemic effect following a single oral administration of SS-ILP to diabetic type 1 and 2 rats at a dose of 25 IU/kg. The oral administration of an insulin solution to type 1 and 2 diabetic rats did not decrease the blood glucose levels, however, a significant glucose reduction was observed in both diabetic rat groups following oral administration of SS-ILP. The strong hypoglycemic effect was observed during the entire study period in both rat groups and blood glucose levels did not return to the initial levels. These observations clearly demonstrate that the SS-ILP is an effective formulation for oral insulin delivery to diabetic rats, irrespective of the diabetes type.

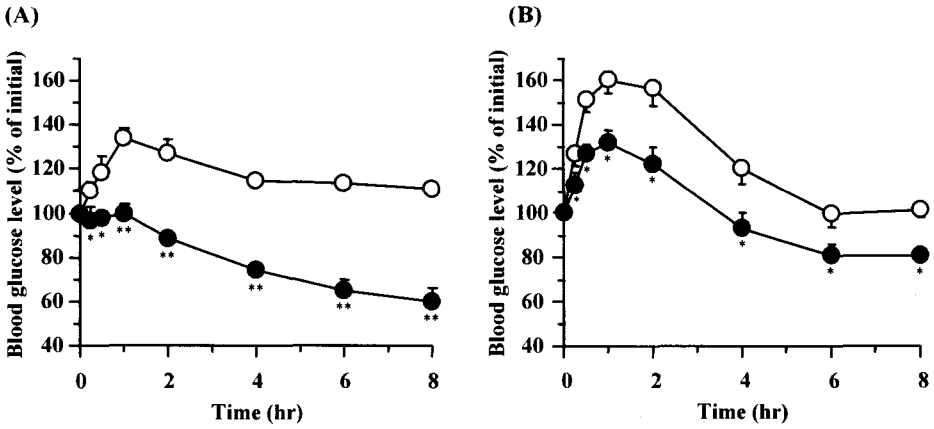

Fig. 11. Changes in blood glucose level versus time profiles following oral administration of SS-ILP (25 IU/kg) in (A) type 1 and (B) type 2 diabetic rats. Each value represents the mean ± S.E. (n=5). Statistically significant difference from control: $p<0.01$,**; $p<0.05$,*. Key: (open circle) insulin solution (control); (closed circle) SS-ILP.

3.4 Hypoglycemic effects following the multiple oral administration of SS-ILP to diabetic rats

In order to ensure the usefulness of the SS-ILP formulations, a multiple oral dosing

study was carried out, as would be needed for a diabetes regimen. The SS-ILP was administered 3 times/day to type 1 and 2 diabetic rats. Figure 12 shows the blood glucose level-time profiles following multiple oral administration of SS-ILP to type 1 diabetic rats. As shown in Fig. 12, SS-ILP significantly suppressed the postprandial rise in blood glucose and showed continuous hypoglycemic effects. In addition, the blood glucose levels prior to each meal could be kept almost the same as the pre-dose values. These results suggest that the multiple oral administration of SS-ILP was highly effective for controlling the glucose level after meals. In contrast, in the insulin solution administration group, glucose levels increased after the meal and did not return to the initial values. Therefore, the pre-dose value prior to the second and the third oral administration of insulin solution was substantially higher than the baseline values.

In the type 2 diabetic rats group, the overall blood glucose levels tended to fluctuate more than those observed in the streptozotocin-induced type 1 diabetic rats group (Fig. 13). However, SS-ILP significantly suppressed the postprandial rise in blood glucose levels in the type 2 diabetic rats group, similarly to the type 1 diabetic rats group.

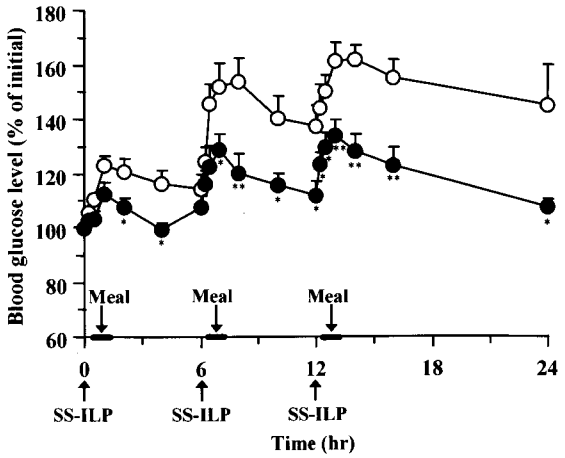

Fig. 12. Changes in blood glucose level versus time profiles in type 1 diabetic rats following multiple oral administration of SS-ILP (25 IU/kg). Each value represents the mean ± S.E. (n=5-10). Statistically significant difference from control: $p<0.01$,**; $p<0.05$,*. Key: (open circle) insulin solution (control); (closed circle) SS-ILP.

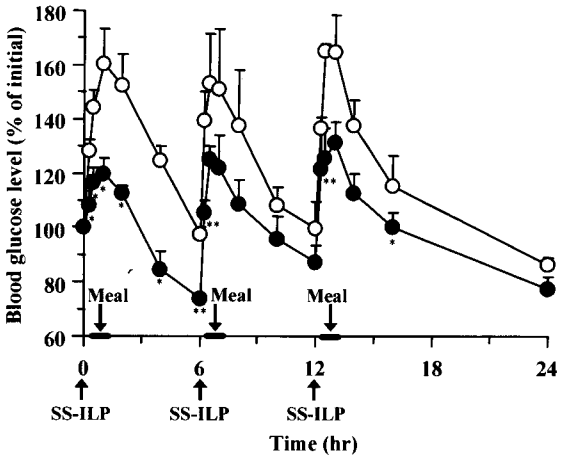

Fig. 13. Changes in blood glucose level versus time profiles in type 2 diabetic rats following multiple oral administration of SS-ILP (25 IU/kg). Each value represents the mean ± S.E. (n=5-10). Statistically significant difference from control: $p<0.01$,**; $p<0.05$,*. Key: (open circle) insulin solution (control); (closed circle) SS-ILP.

As shown in Fig. 12, multiple oral administration of SS-ILP caused a significant decrease of glucose levels compared with control, however the glucose levels at 24 h after administration were slightly higher than the baseline levels. Therefore, in order to avoid increasing the pre-dose glucose levels, an insulin s.c. injection was administered to type 1 diabetic rats together with the oral SS-ILP at the first dosing (Fig. 14). As shown in Fig. 14, co-administration of oral ILP and an insulin s.c. injection strongly suppressed the initial rises of glucose levels after the first meal. In addition, throughout the study period, blood glucose levels could be kept low by only one s.c. injection along with multiple oral SS-ILP administrations.

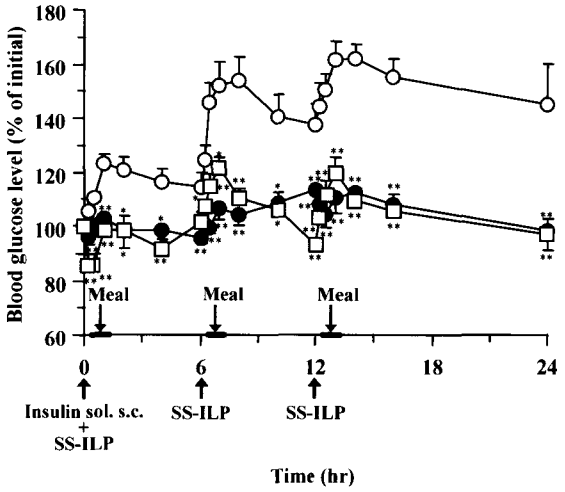

Fig.14. Changes in blood glucose level versus time profiles in type 1 diabetic rats following multiple oral administration of SS-ILP (25 IU/kg) and subcutaneous insulin solution (0.1 IU/kg, only at the first dosing). Each value represents the mean ± S.E. (n=5-10). Statistically significant difference from control: $p<0.01$,**; $p<0.05$,*. Key: (open circle) oral administration of insulin solution (control); (closed circle) subcutaneous administration of insulin solution; (open square) SS-ILP and subcutaneous insulin solution.

4. Discussion

To date, various polymeric carriers have been used to develop peptides and protein drug delivery systems, however, the carriers have not shown sufficient bioavailability when administered by the oral route. In the case of insulin, an oral delivery system which can successfully control blood glucose levels following multiple oral administrations under feeding conditions has not yet been reported. In this chapter, I attempted to identify the optimal formulation of ILP and to prove their potential as an oral insulin carrier in the *in vivo* absorption study.

As shown in Fig. 8, an increase of the EG molar ratio of P(MAA-g-EG) significantly increased the hypoglycemic effect, with administration using the 1:1 molar ratio microparticles of MAA/EG showing the highest PA values (Table 4). These results suggest that the PEG chains in the hydrogels play a critical role in oral insulin delivery. Polyethylene glycol chains are the essential component for exhibiting pH-dependent swelling, since the interpolymer complexes are formed by hydrogen bonding between the carboxylic acid on MAA and the ether group on grafted PEG chains. Lowman et al. reported that PEG chains strongly influence the mesh size of the hydrogel networks [14]. As the EG molar ratio increased, the mesh size significantly decreased. Therefore, an increase in the EG molar ratio provided a network having a small enough mesh size to limit insulin diffusion in low pH environments, while in neutral pH environments it provided a large enough mesh size for insulin to diffuse in and out of the network. In fact, both 4:1 and 1:0 ratios of MAA/EG microparticles released more than 50 % of incorporated insulin in the acidic environment [17], thereby large amount of insulin may then be degraded by proteolytic enzymes in the stomach in this study. In contrast, a 1:1 ratio of MAA/EG

microparticles strongly suppressed insulin release in the acidic environment, which avoided the proteolytic degradation of insulin in the stomach. Insulin could then rapidly be released in the small intestine. This resulted in higher PA values of the 1:1 ratio of MAA/EG microparticles.

Another important factor of PEG chains is the enhancement effect of mucoadhesion of the hydrogels. It was reported that the tethered PEG chains enhanced adhesion to the mucus layers due to interdiffusion and entanglements with mucus layers [18,20]. Therefore, the mucoadhesive effects of a 1:1 ratio of MAA/EG microparticles would be stronger than that of a 1:0 or 4:1 ratio of MAA/EG microparticles. Generally, insulin degradation by pancreatic proteases, such as trypsin and chymotrypsin, occurs in both intestinal fluid and the mucus/glycocalyx layers [1,2]. Therefore, interpenetration of ILP into the mucus/glycocalyx layers might lead to a reduction in proteolytic degradation because insulin is released more closely to the surface of the intestinal epithelial cells.

The bioadhesive capacity of the polymer would also be dependent on particle size. Therefore, it was hypothesized that a smaller size of ILP would cause a greater hypoglycemic effect as compared with larger sized ILPs. As shown in Chapter 1, the SS-ILP, having a particle size less than 53 μm, showed higher mucoadhesion than L-ILP having a particle size between 180-230 μm. In addition, insulin was more rapidly released from SS-ILP than from L-ILP. This implies that the smaller particle size can provide near instant insulin release at the absorption site resulting in a higher local concentration, thereby allowing more insulin absorption. This greatly contributes to the high PA values of SS-ILP in single oral administration studies. The strong hypoglycemic effects of SS-ILP were also demonstrated in a multiple oral

administration study. In fact, this is the first demonstration that oral insulin decreases blood glucose concentration following multiple oral administrations in the presence of food.

Another factor affecting the insulin absorption is the dosing amount of L- and SS-ILP. As shown in Table 5, the PA values following oral administration decreased with an increase in insulin dose, and the highest PA values were obtained at a dose of 10 IU/kg following oral administration of L- and SS-ILP. In this study, insulin dose was adjusted by the amount of ILP. Therefore, rats were administered more amount of the polymer at higher insulin dose. Since the volume of releasing medium strongly influenced the insulin release amount from the microparticles [40], the small intestinal fluid volume might not be enough for completely releasing insulin at higher dose.

5. Conclusions

This study clearly demonstrated that the oral application of SS-ILP in healthy and type 1 and 2 diabetic rats caused significant hypoglycemic effects. In a multiple administration study, SS-ILP significantly suppressed the postprandial rise in blood glucose and showed continuous hypoglycemic effects following 3 times/day oral administration to both diabetic rats groups in the presence of foods. These findings suggest that blood glucose levels of diabetic rats can be effectively controlled by oral SS-ILP administration, and complexation polymer hydrogels may be useful carriers for the oral delivery of peptides and proteins, specially insulin.

Chapter 3

Gastrointestinal transit and mucoadhesive characteristics of complexation hydrogels in rats

1. Introduction

As described in Chapter 1 and 2, the polymer composition and particle size of ILP strongly influenced the oral insulin absorption. In addition, microparticles of diameters of <53 μm (SS-ILP) composed of a 1:1 molar ratio of MAA/EG units showed the most pronounced hypoglycemic effects following oral administration to healthy rats, achieving a 9.5% pharmacological availability compared to subcutaneous insulin injection .

One of the most important attributes of the complexation hydrogels used as vehicles for oral delivery is their ability to adhere to the intestinal mucosa and prolong the residence time of the drug at the site of absorption. It is believed that in these systems, PEG tethers attached to the polymer network act as adhesion promoters to enhance the mucoadhesive behavior of the carriers [18,20]. Favorable interactions of the pendent PEG chains in the polymer networks with the intestinal mucosa may increase the residence time of the carriers in the GI tract. In addition, it was reported that the particle size affected the mucoadhesive properties [28,29]. Thus, smaller size particles tended to adhere more highly to mucus layers than did larger particles [28,29]. However, the mucoadhesive characteristics of the P(MAA-g-EG) microparticles in the GI tract have not been studied *in vivo*. Therefore, the objective of this study was to evaluate the GI transit and mucoadhesive properties of the complexation hydrogels in rats. Particularly, we examined the influence of molar ratio and particle size of the P(MAA-g-EG) hydrogels on the GI transit profiles and mucoadhesive characteristics. In addition, GI transit profiles and mucoadhesive characteristics of P(MAA-g-EG) microparticles was compared with that of polystyrene microparticles as an non-adhesive particles.

2. Experimental section

2.1 Materials

MAA, TEGDMA, and PEGMA were the same as described in Materials of Chapter 1 and 2. PolyFluor® 407, 9-anthracenmethyl methacrylate, and polystyrene yellow green microparticle (45 μm) were purchased from Polysciences Inc. (Warrington, PA, USA). 1-Hydroxycyclohexyl phenyl ketone (Irgacure®-184) was obtained from Ciba-Geigy Co. (Hawthorne, NY, USA). Sodium deoxycholate was purchased from Wako Pure Chemical Industries Co., Ltd (Osaka, Japan). All other chemical used were of reagent grade without further purification.

2.2 Preparation of fluorescently labeled P(MAA-g-EG) microparticles

Fluorescently labeled microparticles were prepared by incorporating PolyFluor® 407 and a fluorescent monomer into the polymer network during the polymerization reaction. Polymer films were prepared by UV-initiated free radical solution polymerization of MAA and PEGMA. The monomers were mixed in appropriate molar ratios to yield solutions with 1:0 and 1:1 ratios of MAA/EG in the gels, henceforth designated as P(MAA-g-EG)(1:0) and P(MAA-g-EG)(1:1), respectively. The fluorescent monomer was added in 0.1 mol% of the total monomer. TEGDMA was used as the crosslinking agent and was added in the amount of 0.75 mol% of the total amount of monomers. The photoinitiator, Irgacure®-184 was added in the amount of 0.1 wt% of the total amount of monomers. To inhibit autoacceleration in the polymerization reaction, monomer mixture was diluted with a mixture of 50 v/v% ethanol and deionized water. Nitrogen was bubbled through the well-mixed solutions for 25 min to remove dissolved oxygen, which could act as a free radical scavenger. The reaction mixtures were

pipetted between glass plates separated by Teflon spacers of 0.9 mm thickness and exposed to UV light (16 mW/cm^2 at 365 nm) under nitrogen environment for 30 min. The ensuing hydrogel films were removed and rinsed for 7 days in deionized water to remove the unreacted monomers and sol fraction. Then, the copolymers were dried u nder vacuum and crushed and sieved to powders with diameters of <53 (SS size) and 150-212 (L size)μm.

2.3 GI transit study

Animal research studies complied with the regulations of the Committee on Ethics in the Care and Use of Laboratory Animals of Hoshi University. Male Wistar rats (180-220 g) were purchased from Sankyo Lab Service Co., Ltd. (Tokyo, Japan). Animals were housed in rooms controlled at 23±1 °C and 55±5 % relative humidity and allowed free access to water and food during acclimatization. Rats were fasted for 48 h prior to the experiment. During the experimental period, rats were housed in cages and given water ad libutum. Rats were restrained in a supine position on a board during administration. Gelatin capsules (Qualicaps® capsule, Shionogi Quolicaps Co., Ltd, Nara, Japan) containing 10 mg microparticles were orally administered using a sonde needle. At 0.5, 1, 2, and 4 h following administration, the rats were sacrificed by sodium pentobarbital overdose, and the stomach and small intestine (divided into three segments) were removed. Each segment was opened lengthwise and the mucus was scraped carefully away using a spatula. The mucus was dissolved in 0.01 w/v% sodium deoxycholate solution. The fluorescence associated with microparticles was measured by a fluorescence spectrophotometer (Mithras LB940, Beltold Japan Co., Ltd., Osaka, Japan) at excitation and emission wavelength of 355 nm and 410 nm

(P(MAA-g-EG) microparticles), and 485 nm and 535 nm (polystyrene microparticles), respectively.

2.4 Transit parameters

The transit of microparticles though the GI tract was evaluated using the kinetic model designed by Akiyama et al. [41], and modified by Sakuma et al. [42]. It was assumed that microparticles were emptied from the stomach and moved through small intestine with first-order kinetics. The gastric emptying rate constant, k_1, was defined as the terminal elimination rate of the particles from the stomach to the small intestine. The intestinal emptying rate constant, k_2, was defined as the terminal elimination rate of the particles from the intestine to the large intestine. Each rate constant was calculated according to the following equation using the non-linear least-squares method with a weight of 1 (MULTI) [43].

$$Rs = 100 \times e^{-k_1 t}$$

$$Rsi = \frac{100 \times k_1}{k_1 - k_2} (e^{-k_2 t} - e^{-k_1 t})$$

Where Rs is the % of the microparticles remaining in the stomach, and Rsi is the % of the microparticles remaining in the small intestine.

2.5 Mucoadhesion study

Male Wistar rats weighting 180-220 g fasted for 24 h were anaesthetized by an i.p. injection of sodium pentobarbital. The rats were restrained in a supine position on the thermostatically controlled board at 37 °C and kept at body temperature. The duodenum was exposed following small midline incision carefully made in the

abdomen, and this segment (10 cm) was cannulated at both ends using polypropylene tubings (4 mm o.d., 2 mm i.d., Saint-Gobain Norton Co., Ltd., Nagano, Japan). These were securely ligated to prevent fluid loss and subsequently, carefully returned to their original location inside the peritoneal cavity. In order to wash the intestinal content, phosphate-buffered saline (PBS; pH 7.4) warmed at 37 °C were circulated through the cannula at 5 mL/min for 4 min using peristaltic pump (PSK-51, Nikkiso Co., Ltd., Tokyo, Japan). Following 1 h resting, 10 mg of microparticles dispersed with 1 mL of PBS solution was directly administered into the loops. At 5 min after administration, PBS at 37 °C was perfused for 10 min at 1 mL/min and the amount of microparticles in the perfusate was calculated by a fluorescence spectrophotometer. Mucoadhesive % was calculated using the following equation.

Mucoadhesive %=(dosing amount–amount of unadhered particle)×100/dosing amount

2.6 Statistical analysis

The results were expressed as the mean ± S.E. For group comparison, an analysis of variance (ANOVA) with a one-way layout was applied. Significant differences in mean values were evaluated by the Student's t-test. A difference was considered to be statistically significant when p value was less than 0.05.

3. Results

3.1 Distribution of P(MAA-g-EG) microparticles in GI tract

The GI transit of the P(MAA-g-EG) microparticles in rats was evaluated and compared with that of polystyrene microparticles as a control. Figures 15 (A) and (B) shows the distribution profiles of polystyrene and SS size of P(MAA-g-EG)(1:1) microparticles in the GI tract of the rats, respectively, at 0.5, 1, 2, and 4 h following oral administration of gelatin capsules containing 10 mg microparticles. After 0.5 h, the P(MAA-g-EG)(1:1) microparticles were mostly located in the stomach, while 30 % of polystyrene microparticles passed though the stomach. After 1 h, more than 60 % of P(MAA-g-EG)(1:1) microparticles had accumulated in the middle and lower segments of the small intestine. As shown in Table 6, more than 90 % of P(MAA-g-EG)(1:1) microparticles existed in the whole GI tract. On the other hand, polystyrene microparticles immediately passed through the middle and the lower part of small intestine, and reached at the colon. Even at 4 h, 25 % of the P(MAA-g-EG)(1:1) micropaticles still located in the GI tract, whereas only 5 % of polystyrene microparticles were in the same region. These results are a strong indication that the P(MAA-g-EG)(1:1) microparticles have strong mucoadhesive characteristics with the intestinal mucosa and remain there for extended periods.

Figures 15 (B) and (C) show GI transit profiles of the P(MAA-g-EG) microparticles containing 1:1 and 1:0 molar ratio of MAA/EG. The P(MAA-g-EG)(1:0) microparticles immediately passed through the stomach and the small intestine. In contrast, the P(MAA-g-EG) microparticles containing 1:1 ratio of MAA/EG remained in the small intestine for extended period and transited slowly to the large intestine. These results indicated that the polymer composition as expressed by the molar ratio of

P(MAA-g-EG) affected the GI transit profile.

GI transit of two different size (SS and L size) of P(MAA-g-EG)(1:1) microparticles was also compared in this study, as shown in Fig. 15 (B) and (D), respectively. Both microparticles passed through the stomach and accumulated in the small intestine slowly, and there are no significant difference in the distribution profiles of L and SS size of P(MAA-g-EG)(1:1) microparticles.

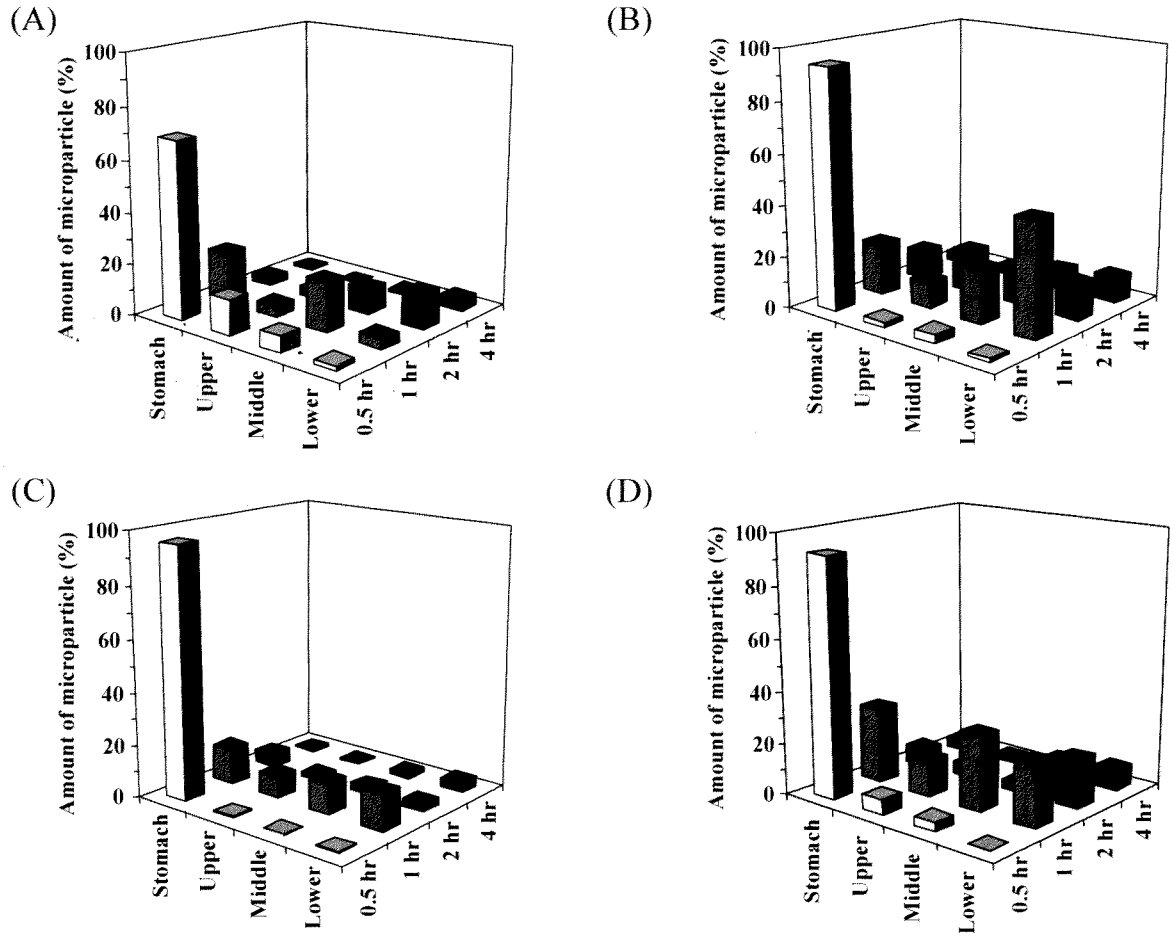

Fig. 15. Distribution profiles of (A) polystyrene, (B) SS size P(MAA-g-EG)(1:1), (C) SS size P(MAA-g-EG)(1:0), and (D) L size P(MAA-g-EG)(1:1) microparticles in the GI tract following oral administration of 10 mg microparticles filled in gelatin capsules. Each column represents mean of three animals.

Table 6.

Recovery % of microparticles in the whole GI tract at 1 h following oral administration

Preparation	Recovery %
P(MAA-g-EG) microparticles	
MAA:EG=1:0 SS size	48.2 ± 11.5
MAA:EG=1:1 SS size	97.7 ± 6.4
MAA:EG=1:1 L size	96.4 ± 3.4
Polystyrene microparticles	47.5 ± 3.6

Each value represents the mean ± S.E. (n=3)

Statistically significant difference between the preparation: $p<0.05$,*, $p<0.01$, **

3.2 Transit parameters of microparticles in the GI tract

Table 7 shows the values of the rate constants obtained by fitting the percentage of the microparticles remaining versus time profiles to the equations using a non-linear least square program, MULTI [43]. The gastric and intestinal emptying rate constants of P(MAA-g-EG)(1:1) were significantly lower than that of polystyrene and P(MAA-g-EG)(1:0) microparticles.

P(MAA-g-EG) microparticles with smaller size had slightly decreased gastric emptying rate constant. In addition, the intestinal emptying rate constant was significantly decreased by virtue of reduction of the particle size.

Table 7.

Kinetic parameters (gastric, k_1, and intestinal, k_2, emptying rate constant) of microparticles in the GI tract

Preparation	k_1 (h^{-1})	k_2 (h^{-1})
P(MAA-g-EG) microparticles		
MAA:EG=1:0 SS size	0.94	1.84
MAA:EG=1:1 SS size	0.88	0.46
MAA:EG=1:1 L size	0.93	0.67
Polystyrene microparticles	1.11	1.34

3.3 Mucoadhesion of microparticles in the intestinal tract

To further understand the mucoadhesive properties of P(MAA-g-EG), the

mucoadhesion of the particles to the duodenal mucosa was evaluated by in situ closed loop technique. Table 8 shows the mucoadhesive characteristics of P(MAA-g-EG)(1:1), P(MAA-g-EG)(1:0) and polystyrene microparticles to the duodenal mucosa. More than 50 % of the polystyrene microparticles were eluted from the duodenum with the PBS solution, while approximately 70 % of the P(MAA-g-EG)(1:1) microparticles remained in the duodenum after PBS perfusion. These results indicated that the P(MAA-g-EG)(1:1) microparticles had the strong mucoadhesive capacities to the intestinal mucosa. In addition, P(MAA-g-EG)(1:1) remained longer in the duodenum compared with P(MAA-g-EG)(1:0). These results indicate that the PEG composition as expressed by the PEG molar ratio of the P(MAA-g-EG) microparticles strongly affects the mucoadhesive properties, and PEG chains possibly act as the anchor to the intestinal mucosa.

In addition, the small size P(MAA-g-EG) microparticles remained more in the intestinal lumen compared with those of large size. These results suggested that particle size of P(MAA-g-EG) microparticles influenced their mucoadhesive capacity, and the smaller particle size of P(MAA-g-EG) exhibited the stronger mucoadhesive characteristics to the duodenal mucosa.

Table 8.

Mucoadhesive properties of P(MAA-g-EG) and polystyrene microparticles in the duodenum.

Preparation	Mucoadhesive %
P(MAA-g-EG) microparticles	
MAA:EG=1:0 SS size	56.3 ± 3.6 *
MAA:EG=1:1 SS size	* 70.4 ± 2.4
MAA:EG=1:1 L size	51.6 ± 3.2 *
Polystyrene microparticles	43.5 ± 6.3

Each value represents the mean ± S.E. (n=3).

Statistically significant difference between the preparation: $p<0.05$,*.

4. Discussion

As shown in Chapter 1 and 2, the P(MAA-g-EG) microparticles could enhance insulin absorption and induce bigger hypoglycemic effect following oral administration. This absorption enhancement of insulin by the hydrogels may be due to the protection of insulin from proteolytic degradation by inhibiting proteases [16] and adhesion to the intestinal mucosa [18,20]. However, the mucoadhesive characteristics of the hydrogels in the GI tract have not been studied. To identify the mucoadhesive characteristics of P(MAA-g-EG) to the GI tract, *in vivo* GI transit and *in situ* mucoadhesion studies were carried out in this chapter.

As shown in Fig.15 (B) and (C), the GI transit of P(MAA-g-EG) containing PEG chains was slower than that of crosslinked PMAA microparticles. Similarly, the mucoadhesive capacity of P(MAA-g-EG)(1:1) microparticles to the duodenal mucosa was higher than that of P(MAA-g-EG)(1:0) microparticles (Table 8). These results imply that the PEG-containing hydrogels exhibit strong mucoadhesive capacities to the intestinal mucosa. Sahlin et al. reported before that the tethered PEG chains enhanced adhesion to the mucus layers due to interdiffusion and entanglement with the mucus layers [19]. Furthermore, Huang et al. [18] showed that the adhesion of P(MAA-g-EG) containing tethered PEG chains was significantly higher at pH 7.4 compared to pH 3.2, indicating that the increased adhesion of the polymer gel was primarily due to the interaction between the PEG chains and the mucus and not due to the hydrogen bonding by the carboxyl groups. From these facts, it was concluded that tethered PEG chains in the P(MAA-g-EG) microparticles could easily interpenetrate and entangle with the mucus layers, which prolong the retention to the GI tract.

Another important factor related to the mucoadhesion is the particle size of the

hydrogels. Recently, a size-dependent particle deposition in the GI tract of rats has been suggested [28,29]. The authors reported an increased adherence for smaller particles in the whole gut. As shown in Figs. 15 (B) and (D), the GI transit profiles of SS and L size were not significantly different. However, the gastric and intestinal emptying rate constant of SS size were decreased compared with L size. Similarly, the particle size of P(MAA-g-EG) microparticles also influenced on the mucoadhesive capacities to the duodenal mucosa (Table 8). These results imply that mucoadhesive capacities to the intestinal mucosa was dependent on the particle size, and smaller size microparticles can easily and deeply interpenetrate into the mucus layers, which show stronger mucoadhesive capacities to the intestinal mucosa.

These results demonstrate that there is a good correlation between mucoadhesive characteristics of P(MAA-g-EG) microparticles and in vivo insulin oral absorption. As shown in Chapter 2, PEG molar ratio and particle size strongly influenced on the insulin oral absorption and the smaller ILP size with MAA:EG=1:1 greatly enhanced insulin oral absorption, achieving a 9.5 % pharamacological availability. From the results in this study, the microparticles of diameters of <53 μm (SS size) composed of a 1:1 molar ratio of MAA/EG show strongest mucoadhesive capacities to the intestinal mucosa. Generally, insulin degradation by pancreatic proteases, such as trypsin and alpha-chymotrypsin, occurs in both intestinal fluid and the mucus/glycocalyx layers [1,2]. Interpenetration of the carriers into the mucus layers might lead to a reduction in proteolytic degradation because insulin is released more closely to the surface of the intestinal epithelial cells. These imply that the P(MAA-g-EG) (MAA:EG=1:1, SS size) microparticles can provide near instant insulin release at the absorption site resulting in a higher local concentration, thereby allowing more insulin absorption.

5. Conclusions

In this study, I demonstrated the ability of tethered PEG chains attached to complexation hydrogels to enhance the retention of the particles in the GI tract. Furthermore, the particle size of P(MAA-g-EG) also influenced the mucoadhesive capacities and smaller size microparticles gave higher mucoadhesiveness. These results indicated that P(MAA-g-EG) microparticles of diameter of <53 μm (SS size) composed of a 1:1 molar ratio of MAA/EG units have the strong mucoadhesive properties to the GI mucosa. This property of the carriers is highly desired in the oral delivery applications, since increasing the residence time of therapeutic peptide and proteins at the targeted site of absorption can significantly improve the fraction of orally administered peptide and protein drugs that reaches the blood circulation.

Chapter 4

Novel mucosal insulin delivery systems based on fusogenic liposomes

1. Introduction

Fusogenic liposomes (FL) are unique delivery vehicles equipped with the envelope glycoprotein of Sendai virus (SeV). FL are prepared by fusing conventional liposomes with inactivated SeV particles, and can deliver encapsulated contents directly and efficiently into the cytoplasm through membrane fusion, with the same mechanism as SeV infection [21-23]. The aim in Chapter 4 was to evaluate the potential of FL to improve the mucosal absorption of peptide and protein drugs. Although it has been reported that FL had a wide range of target cells, their applicability to the intestinal membrane have not yet been established. Therefore, I first investigated the infectivity of SeV to the various intestinal mucosa. The mucus/glycocalyx layers have been known to envelop the surface of the intestinal epithelium and are regarded as an undesirable diffusion barrier that impedes access to absorptive cells of macromolecules and particles [45,46]. As this layer may also impede the accessibility of FL to the intestinal epithelium, the effect of removing the mucus/glycocalyx layers by hyaluronidase pretreatment on membrane fusion was examined. Previous *in situ* absorption study proved that the mucus/glycocalyx layers were successfully diminished without causing detectable cellular damage by hyaluronidase pretreatment [1,2]. The absorption of peptide drugs from various intestinal mucosa with the aid of FL was examined using insulin as a model peptide drug. One of the limiting factors for improving insulin absorption from the intestinal epithelium may be the degradation of insulin in the intestinal cytosol by insulin degrading enzyme (IDE) [47,48]. IDE is the neutral thiol metalloproteinase involved in the intracellular metabolism of insulin in hepatocytes, adipocytes, kidney, muscle cells, intestinal tissue, and other cells [47-49]. Therefore, I investigated whether the co-administration of IDE inhibitor would further

increase the absorption enhancement of insulin by the intestinal administration of FL. Finally, to ensure the safety of FL as an intestinal delivery carrier, the intestinal damage was evaluated by lactate dehydrogenase (LDH) leakage.

2. Experimental section

2.1. Materials

Recombinant human insulin (26.0 units/mg) was the same as described in Materials of Chapter 2. Lyophilized hyaluronidase (EC 3.2.1.35; Type IV-S from bovine testes; MW=56 KDa, 1370 U/mg solid), sodium taurodeoxycholate, and *p*-chloromercuribenzoate (PCMB) were purchased from Sigma-Aldrich Chemical Co., Ltd. (St. Louis, MO, USA). Purified Egg Yolk phosphatidylcholine (PC), L-α-dimyristoyl phosphatidylglycerol (PG) and cholesterol (Chol) were obtained from Nippon Oil and Fats Co., Ltd. (Tokyo, Japan). Polycarbonate membranes (pore size 0.2 μm, Anodisc) were obtained from Whatman plc. (Kent, UK). Sendai virus (Z strain) was prepared in embryonated chicken eggs as described previously [50]. All other chemicals used were of reagent grade without further purification.

2.2. Fusion study of SeV

This research complied with the regulations of the Committee on Ethics in the Care and Use of Laboratory Animals of National Institute of Advanced Industrial Science and Technology, according to the institutional regulations of recombinant DNA experiments. Expression of the green fluorescent protein (GFP) gene carried by recombinant SeV (GFP-SeV) was used to probe the SeV infection (*e.g.*, delivery of the viral genome through membrane fusion), and UV-inactivated virus was used as a negative control. Male Sprague-Dawley rats (180-220 g) were purchased from Tokyo Laboratory Amimals Science Co., Ltd. (Tokyo, Japan). Animals were housed in rooms controlled at 23±1 °C and 55±5 % relative humidity and allowed free access to water and food during acclimatization, but they were fasted for 24 h before experiments. Following

anesthetization by the intraperitoneal injection of sodium pentobarbital (50 mg/kg; Dainippon Pharmaceutical Co., Ltd., Osaka, Japan), the rats were restrained in a supine position on a thermostatically controlled board at 37 °C and maintained body temperature. The ileum, the colon and the rectum were exposed following a small midline incision carefully made in the abdomen, and each segment was cannnulated at both ends using polypropylene tubings (4 mm o.d., 2 mm i.d., Saint-Gobain Norton Co., Ltd., Nagano, Japan). These were securely ligated to prevent fluid loss and subsequently, carefully returned to their original location inside the peritoneal cavity. In order to wash away the intestinal content, phosphate-buffered saline (PBS; pH 7.4) at 37 °C was singly circulated through the cannula at 5 mL/min for 4 min using a peristaltic pump (PSK-51, Nikkiso Co., Ltd., Tokyo, Japan). Subsequently, the intestinal segments were exposed to 1.0 mL of PBS as a control and hyaluronidase solution dissolved in PBS (1.92×10^5 U/mL) for 30 min. After exposure, the segments were carefully rinsed with 20 mL of PBS at 37 °C and the segments were tightly closed following the removal of the cannulation tubing. The SeV suspensions were directly administered to the intestinal segments and the abdomen was sutured. At 16 h following administration, each segment was removed and tissue specimens were prepared. The specimens treated with the tissue-embedding medium O.C.T compound (Tissue-tek®, Sakura Finetek, Inc., Torrance, CA, USA) were frozen in acetone, and 20 μm transverse frozen sections were made in a cryostat (Leica CM 1850, Leica Microsystems, Co., Ltd., Heidelberg, Germany) at -20 °C. Sections were placed on slides, and dried at room temperature. To prevent the bleaching of the fluorescence during microscopic examination, the sections were mounted in anti-fading reagents (Aqua-Poly, Polysciences, Inc. Warrington, PA, USA). Expression of the GFP induced

by GFP-SeV was determined by confocal laser scanning microscopy (Radiance 2100, Bio-Rad Laboratories, Hercules, CA, USA). All photographs were taken with × 100 magnification.

2.3. Preparation and characterization of FL containing insulin

Multilamellar liposomes were prepared by the freezing-thawing method using 120 mg lipids (PC:PG:Chol=4:1:5 molar ratio). The lipid mixtures were dissolved in a small amount of benzene/methanol mixture (95:5, v/v%), and the solvent was rotary evaporated to obtain a thin lipid film. The liposome suspension was prepared by dispersing the dried lipid film with a given amount of insulin solution (either 10 or 30 mg/mL) with or without IDE inhibitor, PCMB (1 mg/mL) using a vortex mixer. The liposomes were frozen rapidly in deep freezer and left to thaw at 37 °C. After 5 cycles of freezing and thawing, unilamellar liposomes were prepared by extrusion through a 0.2 μm polycarbonate membrane and were separated from unencapsulated drugs by ultracentrifugation (40,000 rpm, 90 min). Unilameller FL were prepared as described elsewhere [21-23]. Briefly, unilamelar liposomes were mixed with SeV and incubated at 37 °C for 2 h with shaking. FL was separated from free liposomes and SeV by sucrose density-gradient centrifugation (40,000 rpm, 90 min). The amount of insulin and PCMB loaded into liposomes was determined by HPLC as described in Chapter 1. The encapsulation efficiency of insulin and PCMB into FL was calculated based on the initial and loading amount of drugs. In this study, 3.3 % and 13.0 % of insulin and PCMB in the initial solution was loaded into FL, respectively.

2.4. *In situ* absorption study

This research complied with the regulations of the Committee on Ethics in the Care and Use of Laboratory Animals of Hoshi University. *In situ* absorption study was performed in the same *in situ* system as described above, but except the hyaluronidase treatment was omitted. The ileum, the colon, and the rectum were treated with PBS at 37 °C to wash away the intestinal content. Rats were further left on the board at 37 °C for 1 h to be recovered from the elevated blood glucose levels due to the surgical operations describe above. Following 1 h of rest, the insulin solution or each liposome were directly administered into the ileal, the colonic, and the rectal loops. The dose of all samples was fixed at 5 and 10 IU/kg body weight. During the experiment, a 0.2 mL aliquot of blood was collected from the jugular vein at 0, 5, 10, 15, 30, 60, 120, 180, and 240 min following administration. In order to calculate the efficacy of enteral insulin administration relative to subcutaneous administration, insulin solutions were administered subcutaneously. Insulin solution was prepared by dissolving an appropriate amount of crystalline human insulin in PBS. The insulin subcutaneous dose was 1 IU/kg body weight. Blood samples (0.2 mL) were collected from the jugular vein at the injection before, 5, 10, 15, 30, 60, 120, 180, and 240 min following administration. In order to set the same physical conditions on the rats, the animals receiving s.c. injection were given the same surgical operation as the *in situ* absorption study. The plasma was separated by centrifugation at 13,000 rpm for 1 min and kept in a freezer until insulin concentration analysis. The plasma insulin concentrations were determined on the same day as the absorption study by an immuno-chemiluminometric assay (MLT research limited, Wales, UK) using a microplate luminometer (Mithras LB940, Beltold Japan Co., Ltd., Osaka, Japan). Blood glucose levels were determined using a glucose meter (Novo Assist Plus, Novo Nordisk Pharma Ltd., Tokyo, Japan).

The total area under the insulin concentration curve (AUC) from the time 0 to 240 min was estimated from the sum of successive trapezoids between each data point. The bioavailability was calculated relative to the s.c. injection as described above. The plasma peak level (C_{max}) and the time taken to reach the plasma peak level (T_{max}) were determined from the plasma insulin level-time curves. The area above the blood glucose levels-time curve (AAC) was calculated by a trapezoidal rule. The pharmacological availability (PA) was calculated relative to the insulin s.c. injection, as described above.

2.5. Biochemical evaluation of intestinal damage

The colonic loop from the pretreated segment following the *in situ* experiments as describe above was used here. The colonic segment was treated with PBS (20 mL) at 37 ^{o}C to wash away the intestinal content. PBS (control), 1 % (w/v) sodium taurodeoxycholate (positive control) or FL was administered to the colon and incubated in the segments for 2 h. Then, the colonic loop was washed with 1.0 mL of PBS, and the intestinal fluid was collected. The concentration of lactate dehydrogenase (LDH) in the fluid was determined using a LDH-Test Wako (Wako Pure Chemical Industries, Co., Ltd., Osaka, Japan).

2.6. Statistial analysis

The results were expressed as the mean ± S.D. For group comparison, an analysis of variance (ANOVA) with a one-way layout was applied. Significant differences in the mean values were evaluated using Student's t-test. Differences were considered to be significant when the p value was less than 0.05.

3. Results

3.1. Fusion of SeV to the various intestinal mucosa

Figure 16 shows GFP expression in the various intestinal membranes following the administration of GFP-SeV or UV-inactivated GFP-SeV. GFP expression was clearly detected in each mucosal membrane after treatment with GFP-SeV, but not in those treated with UV-inactivated virus, indicating that the GFP gene was successfully delivered into each mucosal segment through membrane fusion. In addition, the fusion ability of SeV to the large intestine was higher than that to the small intestine. In the ileal segments, hyaluronidase pretreatment significantly enhanced the GFP expression (Figure 16D) compared to those untreated (Figure 16A), whereas it did not affect the GFP expression in the colon (Figures 16B vs. 16E) and the rectum (Figures 16C vs. 16F). These results suggest that the pre-epithelial mucus/glycocalyx layers constitute a barrier for the fusion of SeV with the ileal membrane, but not with the colonic and the rectal membranes.

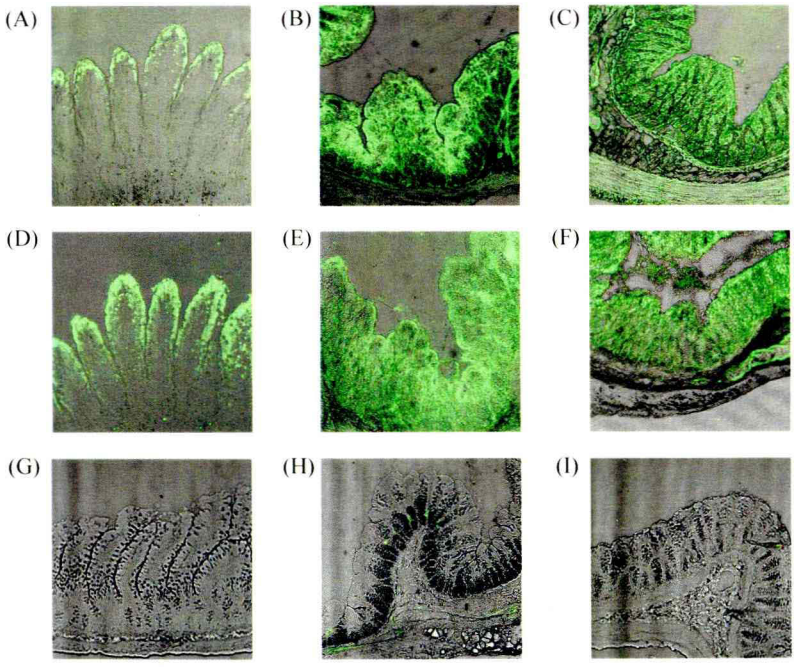

Fig.16. GFP expression in the ileal (A, D, G), colonic (B, E, H), and rectal (C, F, I) mucosa treated with GFP-SeV (A-F) or UV-inactivated GFP-SeV (G-I). Each intestinal segment was pretreated with PBS (A-C, G-I) and hyaluronidase (D-F). Each picture was taken by × 100 magnification.

3.2. Intestinal absorption of insulin following *in situ* administration of insulin-loaded FL

Figure 17 shows the time-course of the plasma insulin and blood glucose levels following *in situ* administration of insulin-loaded FL at a dose of 10 IU/kg into the colonic segments. No apparent insulin absorption and hypoglycemic effect was observed in the insulin solution administration group. Similarly, insulin-loaded liposomes did not enhance insulin absorption, although a slight hypoglycemic effect was observed. In contrast, a marked increase in the plasma insulin levels accompanied by a decrease in the blood glucose levels was observed following the *in situ* administration of insulin-loaded FL into the colonic segments.

Figure 18 shows the insulin absorption following FL administration into the ileal, the colonic, and the rectal segments. In the ileal segment, no apparent insulin absorption and hypoglycemic effect was observed following FL administration, while FL induced the dramatic insulin absorption in the colonic and the rectal segments.

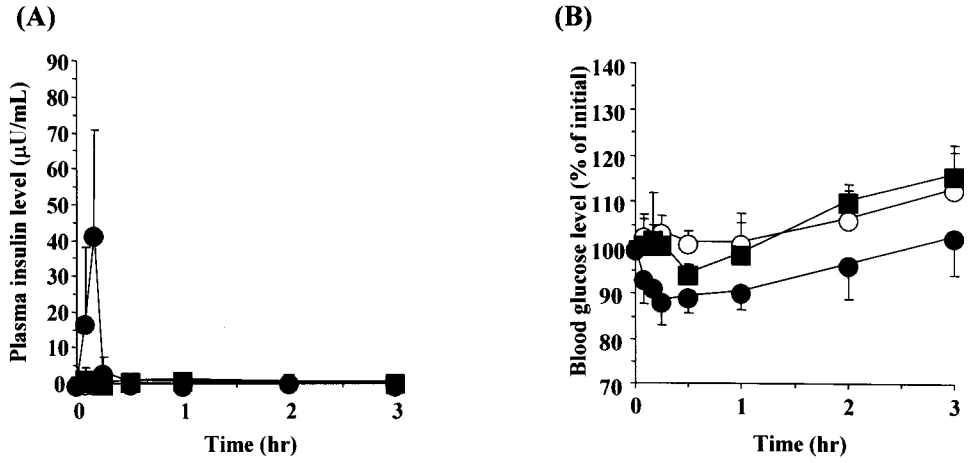

Fig.17. Plasma insulin (A) and blood glucose (B) levels versus time profiles following colonic administration of insulin-loaded FL (10 IU/kg). Each value represents the mean ± S.D. (n=3-4). Key: (open circle) insulin solution (control); (closed square) insulin-loaded liposomes; (closed circle) insulin-loaded FL.

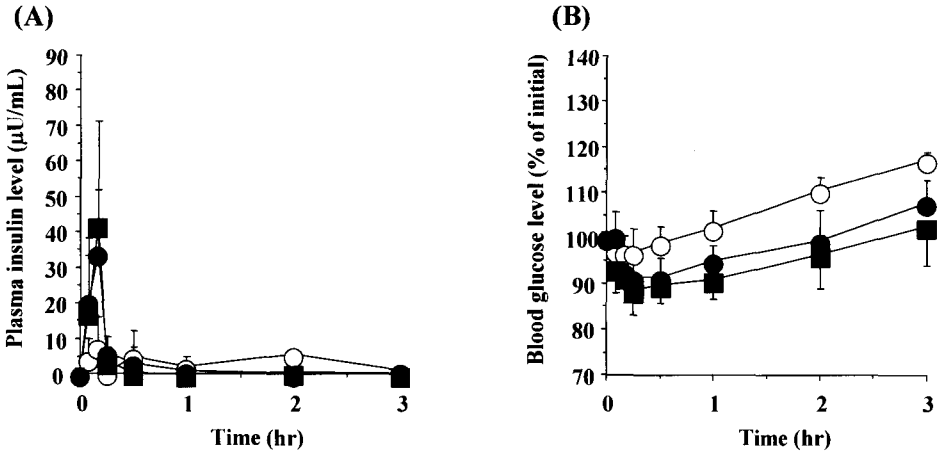

Fig.18. Plasma insulin (A) and blood glucose (B) levels versus time profiles following *in situ* administration of insulin-loaded FL (10 IU/kg) into various intestinal regions. Each value represents the mean ± S.D. (n=3-4). Key: (open circle) ileum; (closed square) colon; (closed circle) rectum.

3.3. Effect of loading amounts on the insulin colonic absorption

Figure 19 shows the effect of the concentration of insulin encapsulated into the FL on the insulin absorption from the colonic segments (A) and hypoglycemic effect (B). The FL loaded with insulin in higher concentration (30 mg/mL) showed stronger insulin absorption enhancement effect than those loaded with insulin in lower concentration (10 mg/mL). These results imply that the average number of insulin molecules encapsulated in a FL particle is a key factor determining the efficacy of insulin delivery by FL.

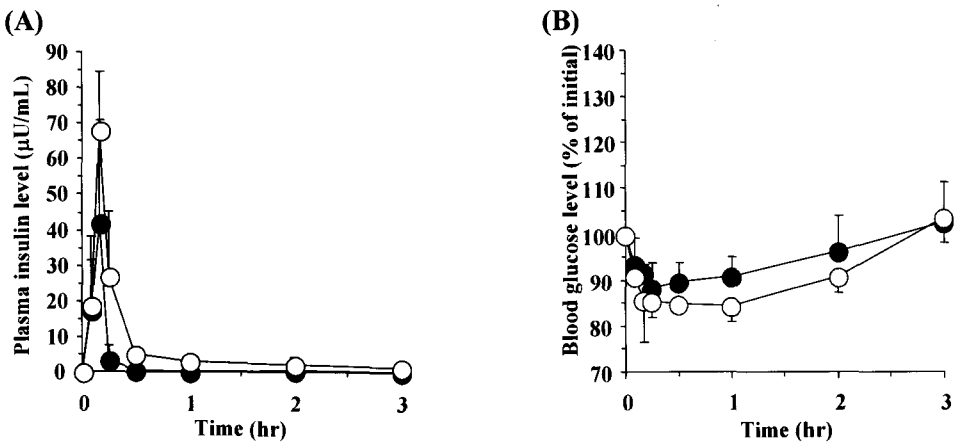

Fig.19. Effect of insulin loading amount into FL on plasma insulin (A) and blood glucose (B) levels. Each value represents the mean ± S.D. (n=3-5). Key: (closed circle) 10 mg insulin-loaded FL; (open circle) 30 mg insulin-loaded FL.

3.4. Effect of IDE inhibitor on the insulin absorption enhancement effect by FL

Figure 20 shows the effect of PCMB co-encapsulated in FL on plasma insulin (A) and on blood glucose (B) levels following the administration of insulin-loaded FL into the colonic segments at a dose of 5 IU/kg. When the insulin solution was co-administered with PCMB, the insulin absorption was not increased. Similarly, both insulin- and PCMB-loaded simple liposomes did not enhance the colonic absorption of insulin. These results indicated that PCMB did not show the absorption-enhancing effect of insulin. In contrast, the FL loaded with both insulin and PCMB together (insulin- and PCMB-loaded FL) further enhanced insulin absorption as compared with insulin-loaded FL. These results demonstrated that the intracellular degradation of insulin by IDE strongly affected the insulin absorption by FL.

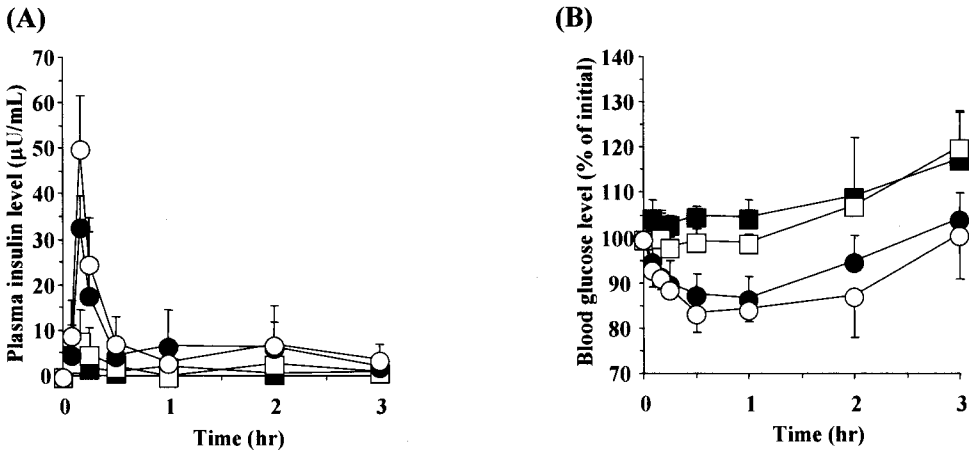

Fig.20. Effect of intra-colonic administration of insulin- and PCMB-loaded FL (5 IU/kg) on plasma insulin (A) and blood glucose (B) levels. Each value represents the mean ± S.D. (n=3-5). Key: (closed square) insulin + PCMB solution (control); (open square) insulin- and PCMB-loaded liposomes; (closed circle) insulin-loaded FL; (open circle) insulin- and PCMB-loaded FL.

Table 9 summarizes the pharmacokinetic parameters of insulin following the colonic administration of insulin-loaded FL. In this study, the pharmacological availability and relative bioavailability were calculated based on the s.c. injection of 1.0 IU/kg of

insulin. Insulin-loaded FL was found to have higher values of pharmacokinetic parameters, C_{max}, AUC, PA, and BA, than that of insulin solution and insulin-loaded liposomes. Furthermore, these parameters were further increased by the addition of IDE inhibitor into the insulin-loaded FL, and their PA and BA values of insulin were greatly improved, up to approximately 16 % and 8 %, respectively.

Table 9.

Pharmacokinetic parameters following the colonic administration of insulin + PCMB solution, insulin- and PCMB-loaded liposomes, insulin-loaded FL, and insulin- and PCMB-loaded FL

Preparation	C_{max} (μU/mL)	T_{max} (h)	AUC (μU·mL^{-1}·h)	PA (%)	BA (%)
Insulin + PCMB solution	7.0 ± 4.5	0.3 ± 0.2	4.3 ± 1.0	0.6 ± 1.1	1.5 ± 0.4
Insulin + PCMB liposomes	11.7 ± 3.5	0.2 ± 0.1	6.4 ± 3.0	0.6 ± 0.9	2.1 ± 1.0
Insulin FL	33.5 ± 6.2 *	0.2 ± 0.1	21.5 ± 13.5	10.1 ± 5.6 *	7.3 ± 4.6
Insulin + PCMB FL	50.2 ± 11.5 **	0.2 ± 0.0	24.7 ± 4.2 **	15.7 ± 7.2 **	8.4 ± 1.4 **

Each data represents the mean ± S.D. (n=3-5).

C_{max}: the plasma peak level; T_{max}: the time taken to reach the plasma peak level; AUC: the area under the curve; BA: Relative bioavailability compared to s.c; PA:Pharmacological availability compared to s.c. Significant difference from the control: $p<0.05$, *, $p<0.01$, **.

3.5. Biochemical characterization of the colonic membrane damage following FL administration

Table 10 shows the LDH leakage following the 2 h administration of FL to the colonic region. LDH was negligibly leaked into the colonic segment, which was similar to the leakage seen in the control group. On the other hand, LDH leakage was significantly induced by the administration of sodium taurodeoxycholate. These data suggest that insulin-loaded FL did not induce the intestinal damage, and the absorption-enhancing effect of insulin-loaded FL was not due to a loss of membranous

barrier function affected by cellular viability.

Table 10.

Lactate dehydrogenase (LDH) leakage following PBS (control), FL, and 1.0 % (w/v) sodium taurodeoxycholate (positive control)

Preparation	LDH leakage (U)
Control	0.40 ± 0.10
FL	0.39 ± 0.18
Sodium taurodeoxycholate	5.13 ± 0.46 **

Each value represents the mean ± S.D. (n=3).

Statistically significant difference from control: $p<0.01$,**.

4. Discussion

The absorption of peptide and protein drugs from the intestine is limited because of enzymatic degradation in the GI tract, high molecular weight and hydrophilicity. For overcoming these limiting factors, various types of liposomes have been used to enhance intestinal insulin absorption; however, bioavailability of the peptide and protein drugs observed by liposome administration was insufficient. In order to improve mucosal insulin absorption by active targeting and delivery, I evaluated the potential of FL as a mucosal insulin carrier. The FL is a delivery system that can introduce the encapsulated materials into the living cells directly and efficiently through the membrane fusion [21-23]. From these characteristics, it would be expected that insulin loaded into the FL would be directly introduced into the intestinal epithelium, thereby increasing the intestinal insulin absorption.

As shown in Fig.16, the SeV can deliver the GFP gene into each mucosal membrane through membrane fusion. SeV membrane fusion was caused by two envelope glycoproteins, hemagglutinating and neuraminidase (HN) and fusion (F) protein [24]. The HN protein is involved in cell binding through attachment of the virus envelope to the cellular receptors containing sialic acid, while the F protein plays a major role in fusion of the envelope with the cell membrane. Sialic acid, the receptor for SeV, is present on most cell types, including the apical surface of intestinal membrane. Therefore, SeV can bind to the sialic acid on the surface of intestinal epithelium and fuses with the cell membrane.

The effects of FL on the insulin intestinal absorption was dependent on the site of the administration (ileum, colon and rectum) (Fig. 18), and was consistent with the results of a fusion study of SeV to the intestinal mucosa using GFP expression as a

marker (Fig. 16). As shown in Fig.16, the fusion ability of SeV to the large intestine was higher than that to the small intestine. In addition, it was found that the mucus/glycocalyx layers of the ileal mucosa affected the membrane fusion of SeV. A possible explanation of the results may be due to the different activities of proteolytic enzymes responsible for the degradation of the SeV envelope glycoprotein in the small and the large intestine. Pancreatic enzyme activities were much stronger in the small intestine than in the large intestine [33]. It has been shown that peptide and protein drugs were degraded by pancreatic enzymes such as trypsin and chymotrypsin, which are believed to reside both in the intestinal fluids and the mucus/glycocalyx layers [51]. Asano et al. reported that the SeV envelope glycoproteins were easily degraded by pancreatic enzymes, such as trypsin and chymotrypsin, and lost their activities of fusion to the cell membrane [52]. Therefore, the SeV glycoproteins may be degraded more readily in the ileal mucus/glyocalyx layers than in the colonic and the rectal mucus/glycocalyx layers, and this may explain the obvious regional differences in the insulin absorption by FL.

It was also demonstrated that the increase of the loading amount of insulin in a single FL was quite effective for facilitating the insulin absorption from the colon (Fig. 19). Accounting that the total number of the FL particles are smaller in the high-loading preparation (30 mg/mL insulin) than low-loading preparation (10 mg/mL) because insulin amount administered into the intestine was kept constant in this experiment, specific absorption of insulin per FL particles are increased over the difference in the concentration of insulin encapsulated. Based on a kinetic and quantitative analysis of the SeV fusion to the cell membrane, the number of SeV (or FL) particles capable of fusing with a single cell was limited by the number of the

absorption site on the cell surface [53]. Therefore, the fusion of FL to the intestinal mucosa might be already saturated even at the low concentration of the FL. This may be one of the limiting factors for the use of FL to the mucosal delivery systems.

Regarding the permeation of insulin into the intestinal epithelium, Bai et al. reported that insulin was highly degraded by IDE in the intestinal cytoplasm and it potentially limits the transpepitheilal transport of insulin [47,48]. In this study, it is observed that in the co-encapsulation of PCMB as the IDE inhibitor further increased FL's enhancement effect of insulin colonic absorption (Fig. 20). This implies that insulin, which was directly introduced into the cytosol by the FL membrane fusion, was strongly degraded by the cytosolic IDE. PCMB, a sulfhydryl-modifying agent, has been used to inhibit the degradation of insulin by IDE in the various tissue cytoplasm [47,48]. In the present study, no absorption enhancing effect was observed following insulin and PCMB solution coadministration and the simple liposomes loaded with both insulin and PCMB together. From these findings, it is suggested that PCMB did not have an absorption enhancing effect, and further increasing the absorption enhancement of insulin was only due to reducing the degradation of insulin in the intestinal cytosol.

Generally, the absorption of insulin from the intestine is limited because of enzymatic degradation in the gastrointestinal tract and low permeability though the intestinal mucosa. To date, various strategies have been used to improve intestinal absorption of insulin, however, mucosal bioavailability of insulin was only improved up to 1~5 % by co-administration with absorption enhancers [27] or enzyme inhibitors [27], and chemical modification [8] in the same in situ loop method used in this study. In addition, some of these approaches exhibited several negative effects such as irritation of the intestinal mucosal membrane and impairment of the membrane barrier. In this

study, we observed that insulin-loaded FL successfully enhanced insulin enteral absorption, achieving approximately 8 % bioavailability (Table 9). The high efficacy of FL in mucosal delivery is attributed to the protection of the peptides by the liposomes and the direct introduction of insulin into the intestinal epithelial cells though the membrane fusion. Insulin loaded into the FL may be protected from the enzymatic degradation in the gastrointestinal tract. In addition, the direct introduction of insulin into the epithelial cells by FL may increase the insulin local concentration in the epithelial cells, and passed though the intestinal membrane without detectable cellular damage (i.e., the absence of LDH leakage). Therefore, our results indicated that the direct insulin delivery across the epithelial membrane by FL is essential for improving the absorption of insulin from the intestine. The high bioavailability of insulin represents potential for mucosal delivery carrier.

5. Conclusions

The present findings suggest that FL enhanced the insulin absorption from the large intestine without causing detectable mucosal damage. The FL's absorption-enhancing effect of insulin mucosal absorption showed a site-specificity because the mucous/glycocalyx layers on the small intestinal mucosa impeded the accessibility of FL to the intestinal mucosa. The absorption-enhancement effect of insulin was strongly influenced by the loading amount of insulin into FL. Insulin absorption was further increased by the co-administration of IDE inhibitor, indicating that the insulin introduced into the epithelium may be degraded by the IDE present in the cytoplasm. These results imply that FL can potentially be developed as a carrier for improving insulin absorption from the large intestine. The FL may offer a novel mucosal delivery method not only for insulin, but for any kind of macromolecules such as proteins and gene, as long as they can be encapsulated into the liposomes. Moreover, it is thought that FL is adapted to the large-scale industrial production [54]. We believe that this technology may lead to the achievement of an ideal delivery system for macromolecular therapeutic drugs.

SUMMARY

The development of oral dosage forms of insulin has been difficult due to inactivation of insulin by proteolytic enzymes in the gastrointestinal (GI) tract, mainly in the stomach and the small intestine, and low insulin permeability through the intestinal mucosa.

One of the promising carriers for oral delivery of insulin is complexation polymer hydrogels composed of crosslinked poly(methacrylic acid) and poly(ethylene glycol). The complexation polymer hydrogels are multi-functional carriers showing high insulin incorporation efficiency, a rapid insulin release in the intestine based on their pH-dependent complexation properties, enzyme-inhibiting effects and mucoadhesive characteristics. Thus, they are potential carriers for insulin delivery via an oral route.

Another promising carrier is fusogenic liposomes (FL), prepared by fusing conventional liposomes with Sendai virus (SeV). FL can deliver encapsulated contents directly and efficiently into the cytoplasm through membrane fusion, with the same mechanism as SeV infection.

In this thesis, to identify an optimal oral formulation for clinical use of insulin, the effect of polymer composition and particle size of insulin loaded polymer (ILP) were investigated in the *in situ* and the *in vivo* experiments. Then, the most promising formulation was selected and subsequently used for *in vivo* multiple oral administration studies using diabetic rats. Furthermore, the potential of the FL to improve the mucosal absorption of insulin from rat intestinal membranes was evaluated in the *in situ* absorption method.

In Chapter 1, insulin absorption from ILPs was studied in the *in sit*u loop system.

The smaller sized microparticles (SS-ILP) showed a rapid burst-type insulin release and higher insulin absorption compared with the microparticles having larger sizes, resulting in greater hypoglycemic effects without detectable mucosal damage. In fact, SS-ILP demonstrated higher mucoadhesive capacity to the jejunum and the ileum than those of L-ILP. Moreover, SS-ILP's enhancement effect of insulin mucosal absorption showed a site-specificity, demonstrating maximum effect at the ileal segment. These results imply that the particle size and delivery site are very important factors for ILP with respect to increasing the bioavailability of insulin following oral administration.

The *in vivo* study of insulin oral absorption by ILP was investigated in Chapter 2. The microparticles of diameters of <53 μm (SS-ILP) composed of a 1:1 molar ratio of methacrylic acid/ethylene glycol units showed the most pronounced hypoglycemic effects following oral administration to healthy rats, achieving a 9.5 % pharmacological availability compared to subcutaneous insulin injection. Their usefulness was also confirmed with both type 1 and 2 diabetic rats groups. In a multiple administration study, SS-ILP significantly suppressed the postprandial rise in blood glucose and showed continuous hypoglycemic effects following 3 times/day oral administration to both diabetic rats groups in the presence of foods. These results indicate that the blood glucose levels of diabetic rats can be effectively controlled by oral SS-ILP administration, and thus SS-ILP would be promising delivery carrier of insulin via the oral route.

In Chapter 3, to clarify the absorption enhancement of insulin by the hydrogels, the GI transit and mucoadhesive characteristics of the hydrogels in the GI tract were investigated. The complexation polymer hydrogels showed strong mucoadhesive capacity and significantly prolonged retention in the GI tract. The ethylene glycol

content and particle size of the hydrogels influenced significantly the GI transit and mucoadhesive capacities. The microparticles composed of polymers prepared from 1:1 ratio of methacrylic acid/ethylene glycol and having diameters of <53 μm showed the strongest mucoadhesive capacity. These results imply that the mucoadhesive characteristics of the hydrogels significantly contributed to improve oral insulin absorption.

In Chapter 4, absorption enhancement effect of FL was evaluated in the *in situ* loop system. Insulin-loaded FL successfully enhanced the insulin absorption and induced a significant hypoglycemic effect following the colonic and the rectal administration without detectable mucosal damage. This enhancing effect of insulin absorption was further improved by increasing the amount of insulin loaded in the FL and by co-encapsulating insulin degrading enzyme (IDE) inhibitor. In contrast, the insulin absorption was not increased by the ileal administration of FL, because the mucus/glycocalyx layers overlayed on the ileal epithelium impede the fusion of FL to the intestinal mucosa.

In conclusion, it is anticipated that SS-ILP and FL are useful carrier for oral insulin delivery. However, the insulin bioavailability was not sufficient yet compared with insulin subcutaneous injection. In order to further improve the insulin intestinal absorption, a combination of other strategies such as permeation enhancer, enzyme degradation inhibitor, and site-specific delivery system might be useful. It is thought that the design of novel pharmaceutical delivery systems and the clarification of their characteristics will lead to the development of effective multifunctional dosage form for oral insulin delivery.

ACKNOWLEDGMENTS

First of all, I would like to express my gratitude and appreciation from my heart to Professor Kozo Takayama and Associate Professor Mariko Morishita for their helpful guidance in my research work and preparing this dissertation.

Secondary, I would like to thank Professor Nicholas A. Peppas (Departments of Chemical and Biomedical Engineering, and Division of Pharmaceutics, The University of Texas at Austin) and Professor Anthony M. Lowman (Department of Chemical Engineering, Drexel University) for providing me polymer and great suggestion in my research work.

Further, I wish to thank Dr. Mahito Nakanishi and Dr. Ken Nishimura (Gene Function Research Center, National Institute of Advanced Industrial Science and Technology) for their helpful assistance in my research work.

Moreover, I would like to thank Professor Tomoko Takahashi and Dr. Mayumi Ikegami (Institute of Medicinal Chemistry, Hoshi University), Assistant Professor Minoru Narita and Ms. Masami Suzuki (Department of Toxicology, Hoshi University) for the suggestion in my research.

Also, I wish to thank Dr. Yasuko Obata, Mr. Yoshinori Onuki and the member of the Department of Pharmaceutics for their kindness and friendship.

I would like to thank Mr. Yoshinobu Aoki, Dr. Koji Nakamura, Dr. Kumi Kawano, Dr. Noriko Ogawa, and Dr. Nikhil J. Kavimandan for their kindness.

In addition, I would like to thank Ms. Aya Handa, Ms. Yuki Sekisawa, Ms. Tomoyo Tsutsumi, Mr. Jumpei Ehara, Mr. Kouichi Ohyama, Ms. Syoko Iwasaki, Ms. Chika Kokeguchi, and Mr. Masato Nishikawa for assistant in my research.

Finally, I will be forever in debt to my family for their support, words and comprehension.

REFERENCES

1. Morishita, M., Aoki, Y., Sakagami, M., Nagai, T., Takayama, K., In situ ileal absorption of insulin in rats: effects of hyaluronidase pretreatment diminishing the mucous/glycocalyx layers, Pharm. Res., 21, 309-316 (2004).
2. Aoki, Y., Morishita, M., Asai, K., Akikusa, B., Hosoda, S., Takayama, K., Regional dependent role of the mucous/glycocalyx layers in insulin permeation across rat small intestinal membrane, Pharm. Res., 22, 1854-1862 (2005).
3. Hoffman, A., Ziv E., Pharmacokinetic considerations of new insulin formulations and routes of administration, Clin. Pharmacokinet., 33, 285-301 (1997).
4. Agarwal, V., Khan M.A., Current status of the oral delivery of insulin, Pharmaceutical Technology, 25, 76-90 (2001).
5. Mesiha, M., Plakogiannis, F., Vejosoth, S., Enhanced oral absorption of insulin from desolvated fatty acid-sodium glycocholate emulsions, Int. J. Pharm., 111, 213-216 (1994).
6. Radwant, M.A., Aboul-Enein, H.Y., The effect of oral absorption enhancers on the in vivo performance of insulin-loaded poly(ethylcyanoacrylate) nanospheres in diabetic rats, J. Microencapsul., 19, 225-235 (2002).
7. Morishita, I., Morishita, M., Takayama, K., Machida, Y., Nagai, T., Hypoglycemic effect of novel oral microspheres of insulin with protease inhibitor in normal and diabetic rats, Int. J. Pharm., 78, 9-16 (1992).
8. Asada, H., Douen, T., Waki, M., Adachi, S., Fujita, T., Yamamoto, A., Muranishi, S., Absorption characteristics of chemically modified-insulin derivatives with various fatty acids in the small and large intestine, J. Pharm. Sci., 84, 682-687 (1995).

9. Kimura, T., Sato, K., Sugimoto, K., Tao, R., Murakami, T., Kurosaki, Y., Nakayama, T., Oral administration of insulin as poly(vinyl alcohol)-gel spheres in diabetic rats, Biol. Pharm. Bull., 19, 897-900 (1996).

10. Damge, C., Vranckx, H., Balschmidt, P., Couvreur, P., Poly(alkyl cyanoacrylate) nanospheres for oral administration of insulin, J. Pharm. Sci., 86, 1403-1409 (1997).

11. Marschutz, M.K., Caliceti, P., Bernkop-Schnurch, A., Design and in vivo evaluation of an oral delivery system for insulin, Pharm. Res., 17, 1468-1474 (2000).

12. Takeuchi, H., Yamamoto, H., Niwa, T., Hino, T., Kawashima, Y., Enteral absorption of insulin in rats from mucoadhesive chitosan-coated liposomes, Pharm. Res., 13, 896-901 (1996).

13. Prego, C., Garcia, M., Torres, D., Alonso, M.J., Transmucosal macromolecular drug delivery, J. Control. Release, 101, 151-162 (2005).

14. Lowman, A.M., Peppas, N.A., Analysis of the complexation/decomplexation phenomena in graft copolymer networks, Macromolecules, 30, 4959-4965 (1997).

15. Lowman, A.M., Cowans, B.A., Peppas, N.A., Investigation of Interpolymer Complexation in Swollen Polyelectroyte Networks by Solid State NMR Spectroscopy, J. Polym. Sci. Polym. Phys., 38 2823-2831 (2000).

16. Madsen, F., Peppas, N.A., Complexation graft copolymer networks: swelling properties, calcium binding and proteolytic enzyme inhibition, Biomaterials, 20, 1701-1708 (1999).

17. Morishita, M., Lowman, A.M., Takayama, K., Nagai, T., Peppas, N.A., Elucidation of the mechanism of incorporation of insulin in controlled release systems based on complexation polymers, J. Control. Release, 81, 25-32 (2002).

18. Huang, Y., Leobandung, W., Foss, A., Peppas, N.A., Molecular aspects of muco- and bioadhesion: tethered structures and site-specific surfaces, J. Control. Release, 65, 63-71 (2000).

19. Lowman, A.M., Morishita, M., Kajita, M., Nagai, T., Peppas, N.A., Oral delivery of insulin using pH-responsive complexation gels, J. Pharm. Sci., 88, 933-937 (1999).

20. Sahlin J.J., Peppas N.A., Enhanced hydrogel adhesion by polymer interdiffusion: use of linear poly(ethylene glycol) as an adhesion promoter, J. Biomater. Sci. Polym. Ed., 8, 421-436 (1997).

21. Kato, K., Nakanishi, M., Kaneda, Y., Uchida, T., Okada, Y., Expression of hepatitis B virus surface antigen in adult rat liver. Co-introduction of DNA and nuclear protein by a simplified liposome method, J. Biol. Chem., 266, 3361-3364 (1991).

22. Hayashi, A., Nakanishi, T., Kunisawa, J., Kondoh, M., Imazu, S., Tsutsumi, Y., Tanaka, K., Fujiwara, H., Hamaoka, T., Mayumi, T., A novel vaccine delivery system using immunopotentiating fusogenic liposomes, Biochem. Biophys. Res. Commun., 261, 824-828 (1999).

23. Kunisawa, J., Masuda, T., Katayama, K., Yoshikawa, T., Tsutsumi, Y., Akashi, M., Mayumi, T., Nakagawa S., Fusogenic liposome delivers encapsulated nanoparticles for cytosolic controlled gene release, J. Control. Release, 105, 344-353 (2005).

24. Okada, Y., Sendai virus-mediated cell fusion, Curr. Top Membr. Transp., 32, 297-336 (1988).

25. Matsuzawa, A., Morishita, M., Takayama, K., Nagai, T., Absorption of insulin using water-in-oil-in-water emulsion from an enteral loop in rats, Biol. Pharm. Bull., 18, 1718–1723 (1995).

26. Yamashita, S., Saitoh, H., Nakanishi, K., Masada, M., Nadai, T., Kimura, T., Effects

of diclofenac sodium and disodium ethylenediaminetetraacetate on electrical parameters of the mucosal membrane and their relation to the permeability enhancing effects in the rat jejunum, J. Pharm. Pharmacol., 39, 621–626 (1987).

27. Morishita, M., Morishita, I., Takayama, K., Machida, Y., Nagai, T., Site-dependent effect of aprotinin, sodium caprate, Na_2EDTA and sodium glycocholate on intestinal absorption of insulin, Biol. Pharm. Bull., 16, 68–72 (1993).
28. Desai, M.P., Labhasetwar, V., Amidon, G.L., Levy, R.J., Gastrointestinal uptake of biodegradable microparticles: effect of particle size, Pharm. Res., 13, 1838-1845 (1996).
29. Lamprecht, A., Schafer, U., Lehr, C.M., Size-dependent bioadhesion of micro- and nanoparticulate carriers to the inflamed colonic mucosa, Pharm. Res., 18, 788-793 (2001).
30. Quan, Y.S., Fujita, T., Tohara, D., Tsuji, M., Kohyama, M., Yamamoto, A., Transport kinetics of leucine enkephalin across Caco-2 monolayers: quantitative analysis for contribution of enzymatic and transport barrier, Life Sci., 64, 1243–1252 (1999).
31. Forbes, B., Wilson, C.G.., Gumbleton, M., Temporal dependence of ectopeptidase expression in alveolar epithelial cell culture: implications for study of peptide absorption, Int. J. Pharm., 180, 225–234 (1999).
32. Bernkop-Schnurch, A., The use of inhibitory agents to overcome the enzymatic barrier to perorally administered therapeutic peptides and proteins, J. Control. Release, 52, 1–16 (1998).
33. Langguth, P., Bohner, V., Heizmann, J., Merkle, H.P., Wolffram, S., Amidon, G.L., Yamashita, S., The challenge of proteolytic enzymes in intestinal peptide delivery, J.

Control. Release, 46, 39-57 (1997).

34. Atuma, C., Strugala, V., Allen, A., Holm, L., The adherent gastrointestinal mucus gel layer: thickness and physical state in vivo, Am. J. Physiol.: Gastrointest. Liver Physiol., 280, G922–G929 (2001).
35. Tanaka, Y., Taki, Y., Sakane, T., Nadai, T., Sezaki, H., Yamashita, S., Characterization of drug transport through tight-junctional pathway in Caco-2 monolayer: comparison with isolated rat jejunum and colon, Pharm. Res., 12, 523–528 (1995).
36. Winne, D., Verheyen, W., Diffusion coefficient in native mucus gel of rat small intestine, J. Pharm. Pharmacol., 42, 517–519 (1990).
37. Schipper, N.G., Varum, K.M., Stenberg, P., Ocklind, G., Lennernas, H., Artursson, P., Chitosans as absorption enhancers of poorly absorbable drugs: 3. Influence of mucus on absorption enhancement, Eur. J. Pharm. Sci., 8, 335–343 (1999).
38. Larhed, A.W., Artursson, P., Bjork, E., The influence of intestinal mucus components on the diffusion of drugs, Pharm. Res., 15, 66–71 (1998).
39. Portha, B., Serradas, P., Bailbe, D., Suzuki, K., Goto, Y., Giroix, M.H., Beta-cell insensitivity to glucose in the GK rat, a spontaneous nonobese model for type II diabetes, Diabetes, 40, 486-491 (1991).
40. Nakamura, K., Murray, R.J., Joseph, J.I., Peppas, N.A., Morishita, M., Lowman, A.M., Oral insulin delivery using P(MAA-g-EG) hydrogels: effects of network morphology on insulin delivery characteristics, J. Control. Release, 95, 589-599 (2004).
41. Akiyama, Y., Nagahara, N., Kashihara, T., Hirai, S., Toguchi, H., In vitro and in vivo evaluation of mucoadhesive microspheres prepared for the gastrointestinal

tract using polyglycerol esters of fatty acids and a poly(acrylic acid) derivative, Pharm. Res., 12, 397-405 (1995).

42. Sakuma, S., Sudo, R., Suzuki, N., Kikuchi, H., Akashi, M., Hayashi, M., Mucoadhesion of polystyrene nanoparticles having surface hydrophilic polymeric chains in the gastrointestinal tract, Int. J. Pharm., 177, 161-172 (1999).
43. Yamaoka, K., Tanigawara, Y., Nakagawa, T., Uno, T.,. A pharmacokinetic analysis program (multi) for microcomputer, J. Pharmacobiodyn., 4, 879-885 (1981).
44. Kisel, M.A., Kulik, L.N., Tsybovsky, I.S., Vlasov, A.P., Vorob'yov, M.S., Kholodova, E.A., Zabarovskaya, Z.V., Liposomes with phosphatidylethanol as a carrier for oral delivery of insulin: studies in the rat, Int. J. Pharm., 216, 105-114 (2001).
45. Frey, A., Giannasca, K.T., Weltzin, R., Giannasca, P.J., Reggio, H., Lencer, W.I., M.R. Neutra., Role of the glycocalyx in regulating access of microparticles to apical plasma membranes of intestinal epithelial cells: implications for microbial attachment and oral vaccine targeting, J. Exp. Med., 184, 1045-1059 (1996).
46. Wang, G., Williams, G.,. Xia, H., Hickey, M., Shao, J., Davidson, B.L., McCray, P.B., Apical barriers to airway epithelial cell gene transfer with amphotropic retroviral vectors, Gene Ther., 9, 922-931 (2002).
47. Bai, J.P., Chang, L.L., Transepithelial transport of insulin: I. Insulin degradation by insulin-degrading enzyme in small intestinal epithelium, Pharm. Res., 12, 1171-1175 (1995).
48. Bai, J.P., Chang, L.L., Effects of enzyme inhibitors and insulin concentration on transepithelial transport of insulin in rats, J. Pharm. Pharmacol., 48, 1078-1082 (1996).

49. Hari, J., Shii, K., Roth, R.A., In vivo association of [^{125}I]-insulin with a cytosolic insulin-degrading enzyme: detection by covalent cross-linking and immunoprecipitation with a monoclonal antibody, Endocrinology, 120, 829-831 (1987).

50. Nakanishi, M., Uchida, T., Sugawa, H., Ishiura, M., Okada, Y., Efficient introduction of contents of liposomes into cells using HVJ (Sendai virus), Exp. Cell Res., 159, 399-409 (1985).

51. Ugolev, A.M., Smirnova, L.F., Iezuitova, N.N., Timofeeva, N.M., Mityushova, N.M., Egorova, V.V., Parshkov, E.M., Distribution of some adsorbed and intrinsic enzymes between the mucosal cells of the rat small intestine and the apical glycocalyx separated from them, FEBS Lett., 104, 35-38 (1979).

52. Asano, K., Murachi, T., Asano, A., Structural requirements for hemolytic activity of F-glycoprotein of HVJ (Sendai virus) studied by proteolytic dissection, J. Biochem., 93, 733-741 (1983).

53. Pedroso de Lima, M.C., Ramalho-Santos, J., Martins, M.F., Pato de Carvalho, A., Bairos, V., Nir, S., Kinetic modeling of Sendai virus fusion with PC-12 cells. Effect of pH and temperature on fusion and viral inactivation, Eur. J. Biochem., 205, 181-186 (1992).

54. Nakanishi, M. Biological and chemical hybrid vectors. In Taira, K., Kataoka, K., Niidome, T. (eds.), Non-viral gene therapy, Springer-Verlag, Tokyo, 2005, pp. 118-132.